Characterization of an eastern U.S. severe air pollution episode using WRF/Chem

E. A. Yegorova,[1,2] D. J. Allen,[3] C. P. Loughner,[1,2] K. E. Pickering,[2,3] and R. R. Dickerson[3]

Received 15 September 2010; revised 3 June 2011; accepted 21 June 2011; published 10 September 2011.

[1] On 8–11 July 2007 the eastern United States experienced a severe heat wave and smog event with maximum temperatures approaching 38°C and maximum 8 h average ozone mixing ratios of 125 ppbv. We examine this episode with observations and numerical simulations using the Weather Research and Forecasting model with online chemistry (WRF/Chem with RADM2). The general features of this severe smog event–a broad area of high pressure, weak winds and heavy pollution, terminated by the passage of a cold front–were well simulated by the model. WRF/Chem underpredicted O_3 maxima by 5–8 ppbv where air quality was poor, usually in the northeast, but overpredicted maxima by up to 16 ppbv where ozone amounts were low, usually in the southeast. Simulated O_3 vertical profiles over Beltsville, Maryland, showed good agreement with ozonesonde measurements, but the model boundary layer was too deep on 9 July, contributing to the low bias over this region. The representation of NO_x chemistry in RADM2 may lead to an underestimation of NO_x lifetime and is likely partially responsible for low O_3 biases in the most polluted area in the northeast. To simulate the maximum effect of nighttime multiphase NO_y loss, we set the N_2O_5 heterogeneous hydrolysis reaction rate constant to zero. This increased the mean bias outside the area of highest ozone concentration but substantially improved O_3 and NO_y over most of the domain, especially in smoggy areas such as the rural, Pinnacles site.

Citation: Yegorova, E. A., D. J. Allen, C. P. Loughner, K. E. Pickering, and R. R. Dickerson (2011), Characterization of an eastern U.S. severe air pollution episode using WRF/Chem, *J. Geophys. Res.*, *116*, D17306, doi:10.1029/2010JD015054.

1. Introduction

[2] The mid-Atlantic region faces unhealthy levels of ozone several times each summer. The 7–11 July 2007 episode was one of the worst air quality events recorded in the mid-Atlantic region in the past decade during which 8 h maximum ozone mixing ratios in northeastern Maryland reached 125 ppbv. Such high O_3 8 h maxima are the first to occur in Maryland since emissions in 22 eastern states were reduced substantially beginning in 2003–2004 due to implementation of the NO_x State Implementation Plan (SIP) Call [*Bloomer et al.*, 2009; *Frost et al.*, 2006].

[3] The ability to predict lower-tropospheric ozone in a region of high population density such as the mid-Atlantic is important due to the adverse impacts of ozone on human health. Areas downwind of Washington, D. C., Baltimore, Philadelphia, and New York City report the highest summertime O_3 concentrations in the region. Vehicle emissions of O_3 precursors, NO_x and volatile organic compounds (VOCs) and transport of power plant generated NO_x from the Ohio River Valley contribute to O_3 production. During the 7–11 July 2007 smog episode the heat island effect in downtown Washington, D. C., contributed to higher O_3 mixing ratios downwind in Baltimore, Maryland [*Zhang et al.*, 2009]. *Loughner et al.* [2011], showed that the Chesapeake Bay breeze can cause buildup of pollutants northeast of Baltimore, Maryland, but that this phenomenon cannot be resolved by models with resolution greater than about 5 km. This event ended on 11 July as thunderstorms and a frontal passage vented the Planetary Boundary Layer (PBL) and increased pollutant export from the east coast of the United States thus turning this regional air quality problem into a hemispheric pollution problem.

[4] In this paper, the Advanced Research WRF (ARW) core version 3.1.1 of the Weather Research and Forecasting model with chemistry module (WRF/Chem) [*Grell et al.*, 2005] was used to study the 7–11 July 2007 smog episode. The performance of this regional air quality model (using RADM2 [*Stockwell et al.*, 1990] chemical mechanism) was evaluated with a focus on simulating O_3 and its precursors. WRF/Chem calculated trace gases and meteorological parameters were compared to ground observations and ozonesonde profiles. In a follow-up paper, we will use WRF/Chem to investigate the ability of satellite instruments to detect signatures of the July 2007 smog event from space.

[1]Earth System Science Interdisciplinary Center, University of Maryland, College Park, Maryland, USA.
[2]NASA Goddard Space Flight Center, Greenbelt, Maryland, USA.
[3]Department of Atmospheric and Oceanic Science, University of Maryland, College Park, Maryland, USA.

Copyright 2011 by the American Geophysical Union.
0148-0227/11/2010JD015054

Table 1. WRF/Chem Standard (E_BASE) Configuration Options

Atmospheric Processes	WRF/Chem
Radiation	LW: RRTM; SW: Goddard
Surface layer	Monin-Obukhov
Land surface model	Noah
Boundary layer	YSU
Cumulus	Grell 3D ensemble
Microphysics	Lin
Photolysis	Fast-J
Eddy diffusion	Smagorinsky first-order closure
Meteorological initial and boundary conditions	NARR
Chemical initial and boundary conditions	MOZART-4
Dry deposition scheme	Wesely
Chemical mechanism	KPP RADM2

[5] Numerical prediction models are routinely used for the purpose of forecasting surface pollutant concentrations at specific locations [e.g., *Ryan et al.*, 2000] (http://www.nws.noaa.gov/ost/air_quality/). Regional models tend to underestimate high ozone values. This high bias causes a problem for operational air quality forecasts. PBL height biases, lateral boundary condition assumptions, and deficiencies in chemical mechanism and emissions can contribute to model uncertainty.

[6] Simulations with regional air quality models such as CMAQ and WRF/Chem have been useful for identifying the processes responsible for biases between modeled and observed O_3 and precursors. *Zhang et al.* [2006] linked underprediction of 1 h O_3 daily maxima on high O_3 days to overestimated planetary boundary layer depth. *Cai et al.* [2008] found that deficiencies in the CB-IV chemical mechanism can cause underestimation of NO_z ($NO_z = NO_y - NO_x$) removal and OH concentrations, key contributors to ozone production. *Castellanos et al.* [2011] showed that O_3 underprediction in CMAQ may be due to too quick removal of NO_x in the CB-IV mechanism and to problems with vertical mixing. Similarly, *Henderson et al.* [2011] found that seven chemical mechanisms (including CB05 and RACM2) converted NO_x to HNO_3 too rapidly and, consequently, underrepresented NO_2 by at least 30%. *Gilliland et al.* [2008] showed that CMAQ underpredicts NO_x above the PBL. *Yu et al.* [2007], in a regional air quality modeling simulation with the Eta-CMAQ model performed for the International Consortium for Atmospheric Research on Transport and Transformation (ICARTT) study, found that the model reproduced O_3 vertical distributions at low altitudes, but overestimated O_3 above 6 km due to biases in the lateral boundary conditions and a relatively coarse vertical resolution. *Grell et al.* [2005], in WRF/Chem simulations for the summer of 2002 NEAQS field study in the northeast United States, showed reduction in model mean bias and root mean square error in an experiment changing leaf temperature, which determines biogenic emissions of isoprene, important for O_3 formation.

2. WRF/Chem Simulation

[7] The Weather Research and Forecasting model with online chemistry is a mesoscale numerical weather prediction system designed both for atmospheric research and operational forecasting. This numerical modeling system is "online" in the sense that all processes affecting the gas phase and aerosol species calculation are done in step with the meteorological dynamics [*Grell et al.*, 2005].

[8] WRF/Chem simulations were nested with a 36 × 36 km outer domain and a 12 × 12 km inner domain. The outer domain has 170 × 103 mass points covering the conterminous United States, and the inner domain has 169 × 169 mass points extending from the Midwest to Atlantic Ocean, including the mid-Atlantic region of the United States. There are 32 vertical layers with 10 layers below 900 hPa. The depths of the lowest 10 layers are 2 hPa, 3 hPa, 5 hPa, 6 hPa, 10 hPa, 11 hPa, 15 hPa, 18 hPa, 22 hPa, and 26 hPa. The spacing of the vertical layers increases to about 30–50 hPa from the middle troposphere to the top of the domain (at 100 hPa). The model was initialized on 6 July at 00:00 UTC and run for 7 days.

[9] Standard model configuration (E_BASE) options are listed in Table 1. Emissions were processed using the Sparse Matrix Operator Kernel Emissions (SMOKE) Modeling System with 2007 Continuous Emissions Monitoring Systems (CEMS) measurements and projected 2009 emissions (closest available to 2007) for all sources from the U.S. Regional Planning Offices (RPO). More information on the emissions used in this study is available at http://www.marama.org/reports/MANEVU_Emission_Projections_TSD_022807.pdf. Initial and boundary conditions for the meteorological parameters were taken from the North American Regional Reanalysis (NARR). Initial and boundary conditions for trace gas and particulate species were taken from the global MOZART-4 model with output at 6 h time intervals provided by Louisa Emmons (NCAR) [*Emmons et al.*, 2010].

[10] Objective Analysis (OBSGRID) nudging techniques were used to minimize the accumulation of model errors and preserve mesoscale circulations within the model. OBSGRID nudging improves initial and boundary conditions by combining high-resolution upper level (i.e., rawinsonde, aircraft) and surface observations with global analysis fields [*Wang et al.*, 2009]. OBSGRID analysis is an important option for lowering analyses error and generating more accurate meteorological data for air quality simulations.

[11] To investigate the causes of biases between model and measured O_3 and NO_y species we also performed three sensitivity experiments, as follows.

[12] The first sensitivity experiment is termed E_FDDA. In addition to E_BASE configurations we included the Four-Dimensional Data Assimilation (FDDA) analysis nudging technique. Temperature, water vapor, and winds were nudged toward NARR analysis fields for the outer 36 km domain. This simulation investigates the effects of using additional meteorological analysis nudging on chemical fields.

[13] Another sensitivity experiment is E_DRYDEP. Underestimated dry deposition velocities can cause overprediction of nighttime O_3 in the model. *Wu et al.* [2011] evaluated WRF/Chem Wesely dry deposition module and Noah-GEM model against direct observations in central Massachusetts. They found that WRF/Chem Wesely dry deposition scheme underestimates O_3 dry deposition velocities for nighttime and morning hours. Similarly, *Allen et al.* [2009] showed that Wesely scheme dry deposition velocities (<0.2 cm/s) over eastern United States are lower than M3DRY dry deposition velocities in CMAQ (<0.4 cm/s). Typically, dry deposition velocities can be as large as 1 cm/s

for exposed soil surfaces, 0.5 cm/s for deciduous forests for well mixed conditions, and 0.1 cm/s for wet soils and soils with little organic matter [*Wesely and Hicks*, 2000]. To test the sensitivity of nighttime model O_3 amounts to uncertainties in dry deposition velocities, we doubled O_3 dry deposition velocities over all surfaces within the domain.

[14] The final sensitivity experiment is E_ CHEM. The NO_x removal path by heterogeneous reaction of N_2O_5 to form nitric acid (reaction (1)) is likely overestimated in RADM2. Organic coatings on aerosols may substantially reduce the accommodation coefficient [*Brown et al.*, 2006] and allow some N_2O_5 to return to NO_x via thermal degradation (reaction (2)).

$$N_2O_5(g) + H_2O(aq) \rightarrow 2HNO_3(aq) \quad (1)$$

$$N_2O_5 \rightarrow NO_2 + NO_3 \quad (2)$$

The default WRF/Chem chemical mechanism (RADM2), used in our simulation, does not include the influence of two potentially important reactive nitrogen reservoirs: organonitrates ($RONO_2$, including isoprene nitrates) and nitryl chloride ($ClNO_2$). Heterogeneous reactions of N_2O_5 can lead to two different products: HNO_3 (reaction (1)) or $ClNO_2$:

$$N_2O_5(g) + Cl^-(aq) \rightarrow ClNO_2(g) + NO_3^-(aq) \quad (3)$$

When HNO_3 is created, NO_x is lost and the O_3 production cycle is stopped. When $ClNO_2$ is the product, NO_2 is regenerated in the morning hours allowing production of O_3 to continue [*Thornton et al.*, 2010]:

$$ClNO_2 + h\nu \rightarrow Cl + NO_2 \quad (4)$$

The formation of $ClNO_2$ (reaction (3)) may short circuit the conversion of NO_x to NO_3^-, even great distances from the ocean [*Thornton et al.*, 2010]. The chlorine content of the atmosphere over the eastern United States is not known, but it is likely higher than in Colorado [*Thornton et al.*, 2010]. The short lifetime (~30 min) of $ClNO_2$ during daylight hours means that N_2O_5, even if involved in heterogeneous reaction, can be returned to NO_2 (reaction (3)). Both of these processes (as well as the recycling of NO_x through organonitrates) extend the lifetime of NO_x. If 100% of the N_2O_5 formed were returned to NO_x, either because it is recycled through $ClNO_2$ or because it does not react with aerosols in the first place, then the heterogeneous loss is effectively turned off. To test the maximum possible impact of these reactions on ozone, we set the rate coefficient for reaction (1) to zero in experiment E_CHEM. This change should increase O_3 in the northeast United States, by extending the lifetime of NO_x and its availability for O_3 formation.

3. In Situ Observations

[15] Observations from rural and urban sites are used to evaluate the model's performance in simulating this major smog event. Domain-wide model output was evaluated using ozone observations from the Air Quality System (AQS), an Environmental Protection Agency (EPA) program that collects hourly near-real-time surface pollutant observations from several hundred stations across the U.S. AQS data are available at http://www.epa.gov/ttn/airs/airsaqs/. Detailed air quality evaluation was performed using data from an AQS site at Aldino, Maryland (suburban, 39.6°N, 76.2°W); Pinnacle State Park, New York (rural, 42.1°N, 77.2°W, elev. 504 m) [*Schwab et al.*, 2009]; Great Smoky Mountains, Tennessee (rural, 35.6°N, 83.9°W, elev. 793 m) (data available from http://www.nature.nps.gov/air/Monitoring/MonHist/index.cfm); and Southern Aerosol Research and Characterization (SEARCH) sites in Atlanta, Georgia (urban, 33.8°N, 84.4°W) and Yorkville, Georgia (rural, 33.9°N, 85.0°W) (data available at http://www.atmospheric-research.com/studies/search/). The vertical extent of the polluted air is analyzed using Beltsville, Maryland, ozonesondes [*Yorks et al.*, 2009].

4. Ozone Episode During 7–11 July 2007

[16] Figures 1 and 2 depict surface analysis and model synoptic events, respectively, for 6–12 July 2007. According to the National Centers for Environmental Prediction (NCEP) surface analysis maps, a cold frontal system moved off the East Coast on 6 July 2007 12:00 UTC (Figures 1a and 2a), shifting winds to northwest and decreasing humidity. On 7 July 2007 a high-pressure system, centered over the Ohio River Valley and the Great Lakes area, generated high temperatures, clear skies, and plentiful sunlight, and the onset of ozone production. Maximum temperatures reached 30°C and no precipitation was observed. By 8 July the high pressure moved eastward and a midlatitude cyclone began forming over the Great Lakes (Figures 1b and 2b). Maximum temperatures remained near 30°C in the mid-Atlantic region. High temperatures, sunny skies, and moderate southwest winds set the stage for strong photochemical ozone formation. As the low moved to the northeast over Canada, the anticyclone off the southeast U.S. coast moved over the mid-Atlantic region. On 9 and 10 July, temperatures in the mid-Atlantic region reached 35–37°C. GOES-12 infrared image on 19 July 18:00 UTC shows clear sky conditions in the Washington/Baltimore metropolitan area (Figure 3). Sunny, nearly stagnant conditions, with weak surface winds from the southwest, contributed to the accumulation of ozone (Figures 1c and 2c). On 10 and 11 July a surface trough was aligned just east of the Appalachian Mountains (Figures 1d and 1e); large-scale southwest flow dominated along the eastern seaboard, transporting pollutants from the southeast toward New England. The model is in agreement with the surface analysis as to the location of the isobars (Figures 1e and 2e). The cold front associated with the midlatitude cyclone near James Bay pushed through the Baltimore Washington Metropolitan area around 03:00 UTC on 12 July 2007 (Figures 1f and 2f). The smog event ended as the cold front brought cleaner, cooler air into the region. Overall, WRF/Chem satisfactorily simulated the synoptic circulation patterns that contributed to the July 2007 smog episode in the mid-Atlantic region.

5. Model Comparison to AQS Surface Observations

5.1. Characteristics of Simulated Ozone

[17] The WRF/Chem simulation is evaluated against surface ozone monitoring stations. For each day of the simu-

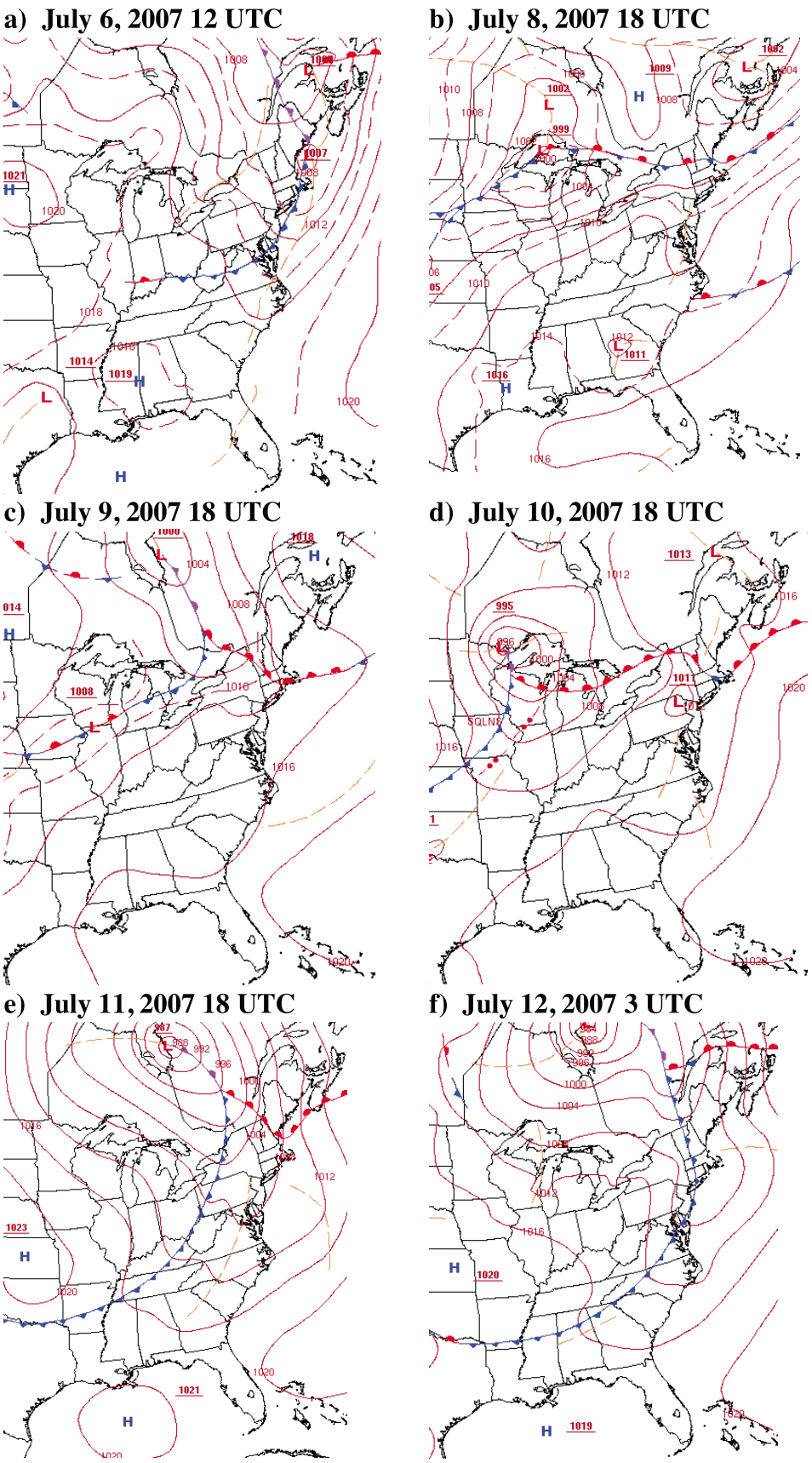
a) July 6, 2007 12 UTC
b) July 8, 2007 18 UTC
c) July 9, 2007 18 UTC
d) July 10, 2007 18 UTC
e) July 11, 2007 18 UTC
f) July 12, 2007 3 UTC

Figure 1

lation, 8 h maximum surface ozone fields were calculated and interpolated to the location of AQS measurements within the nested domain. On 6 July, surface stations were reporting ozone values in the moderate 55–65 ppbv range in the Baltimore–Washington, D. C., region and New England states (Figure 4a). WRF/Chem shows high ozone off the coast of New England states, visible in the AQS coastal measurements extending from Virginia to Massachusetts (Figure 5a). North Carolina, South Carolina, Georgia and Tennessee also reported increased ozone: remnants of an earlier 4–5 July pollution episode. The onset of increased photochemistry and stagnation associated with the high-pressure system is visible in the gradual increase of surface ozone predominantly in the northeast United States in both observations (Figures 4b–4e) and the model (Figures 5b–5e) from 7–10 July. On 9 July AQS 8 h maximum ozone peaked at 100–125 ppbv along the I-95 interstate corridor, from the Washington-Baltimore metropolitan area to Boston. On this day, the model correctly simulates the spatial distribution of the ozone peak along I-95 north of Maryland, but the peak 8 h maximum values are underpredicted by 20–25 ppbv. On 10 July the model underpredicts O_3 distributions by 10–23 ppbv along the Ohio River Valley, where a warm front passed. At the peak of the smog episode in the northeast, the southeast U.S. air quality conditions range from good to moderate ($O_3 < 65$ ppbv). On 11 July, both observations and the model show good air quality conditions following frontal passage across the region.

[18] Table 2 examines daily mean biases (MB) over two regions: northeast U.S. states (Maryland, Delaware, Pennsylvania, New Jersey, and New York) and southeast (North Carolina, South Carolina, Georgia, Alabama, and Mississippi) for the E_BASE and E_FDDA simulations. Opposing regional biases exist in the northeast and southeast in E_BASE and E_FDDA simulations. Overall, WRF/Chem (E_BASE) underpredicts O_3 in the northeast by as much as 7 ppbv and overpredicts O_3 in the southeast by 6 to 11 ppbv. Most of the high regional bias in the southeast is for observed O_3 mixing ratios less than 40 ppbv (Table 3), about 45% of observations in this range. The high bias on days when 8 h maximum was observed to be in the 40–60 ppbv range, was comparable for northeast and southeast (3.68 ppbv and 4.82 ppbv). On average, for poor air quality conditions (50% of northeast sites and 11% of southeast sites), the model underpredicts O_3 by 5–8 ppbv. Generally, low biases are driven by daytime underprediction of peak O_3 concentrations ($O_3 >$ 60 ppbv), while high biases are due to overprediction of O_3 amounts during clean air conditions ($O_3 < 40$ ppbv). Results of sensitivity runs targeting model deficiencies in NO_x recycling and dry deposition velocities are discussed in section 6.

[19] WRF/Chem with additional nudging (E_FDDA) simulated 8 h maximum O_3 is slightly better on 8 and 9 July in the northeast with a low bias of 3–4 ppbv (Table 2). But 10 and 11 July O_3 mean biases exceed 11 ppbv in the northeast. FDDA analysis nudging increases mean bias in southeast United States by 2–18 ppbv leading to mean O_3 biases of 17–24 ppbv.

[20] Analysis of E_BASE and E_FDDA soil and 2 m temperature, PBLH, 6 h accumulated precipitation and surface winds and pressure showed discrepancies in location and strength of convective storms. In general in the southeastern United States, E_FDDA does not capture the spatial extent of cloudiness associated with convection, underpredicts accumulated precipitation amounts and soil moisture, and overpredicts 2 m temperature in comparison with E_BASE and NARR reanalysis. The increased temperatures and reduced occurrence of convection lead to lower cloud fraction, increased photolysis rates, and more O_3 production in the E_FDDA simulation. Previous photochemical modeling studies conducted for central California have also shown that the photochemical model performance does not necessarily improve when the meteorological fields are generated with FDDA [*Tanrikulu et al.*, 2000; *Umeda and Martien*, 2002]. Our results highlight the sensitivity of photochemical O_3 production during this episode to model-generated temperature and solar radiative flux.

5.2. Statistical Analysis

5.2.1. Discrete Statistics

[21] A scatterplot of the modeled and observed 8 h O_3 daily maxima at monitoring sites within the 12 km nested domain during 6–11 July 2007 is shown in Figure 6. The calculated regression line has a slope of 0.53 and intercept of 25.0 ppbv with a correlation coefficient of 0.70. WRF/Chem overestimates low O_3 values and underestimates high values. Previous studies evaluating other regional models, such as CMAQ, HYSPLIT, and MM5-Chem produced similar agreement with observations [e.g., *Kang and Elder*, 2005, *Mao et al.*, 2010, *Gilliland et al.*, 2008, *Godowitch et al.*, 2008, *Castellanos et al.*, 2011]. Figure 7 shows the distribution frequency of observed and simulated 8 h O_3 daily maxima. Observed 8 h O_3 daily maxima ranged from 9 to 125 ppbv, with a peak frequency of occurrence of 12% within the 50–55 ppbv bin. Modeled 8 h O_3 daily maxima were within the 22–92 ppbv range, with a peak frequency of 17% centered at 55–60 ppbv bin. Six percent of AQS measurements and 3% of model forecasts were in exceedance of the NAAQS 8 h maximum ozone standard of 75 ppbv. The model underpredicts the frequency of 8 h maximum ozone mixing ratios less than 40 ppbv and greater than 65 ppbv, but overestimates the frequency in the 40–65 ppbv range. Model O_3 forecasts less than 40 ppbv generally occurred in southern states, rural areas west of the Appalachian Mountains, and northern New England states; forecasts greater than 65 ppbv occurred in urban areas along I-95 corridor and in the Ohio River Valley. Forecasts between 40 ppbv and 65 ppbv occurred across the domain. This category included high O_3 biased model forecasts in the southeast United States on days of good air quality and low O_3 biased forecasts in the northeast United States on days of poor air quality.

Figure 1. NOAA North American analysis and sea level on (a) 6 July 2007 12:00 UTC, (b) 8 July 2007 18:00 UTC, (c) 9 July 2007 18:00 UTC, (d) 10 July 2007 18:00 UTC, (e) 11 July 2007 18:00 UTC, and (f) 12 July 2007 03:00 UTC, contoured by 4 hPa. Surface trough is indicated with a dashed brown line. Note the widespread high-pressure system on 9 July, lee-side trough on 10 July, and approaching cold front on 11 July, ending the smog episode.

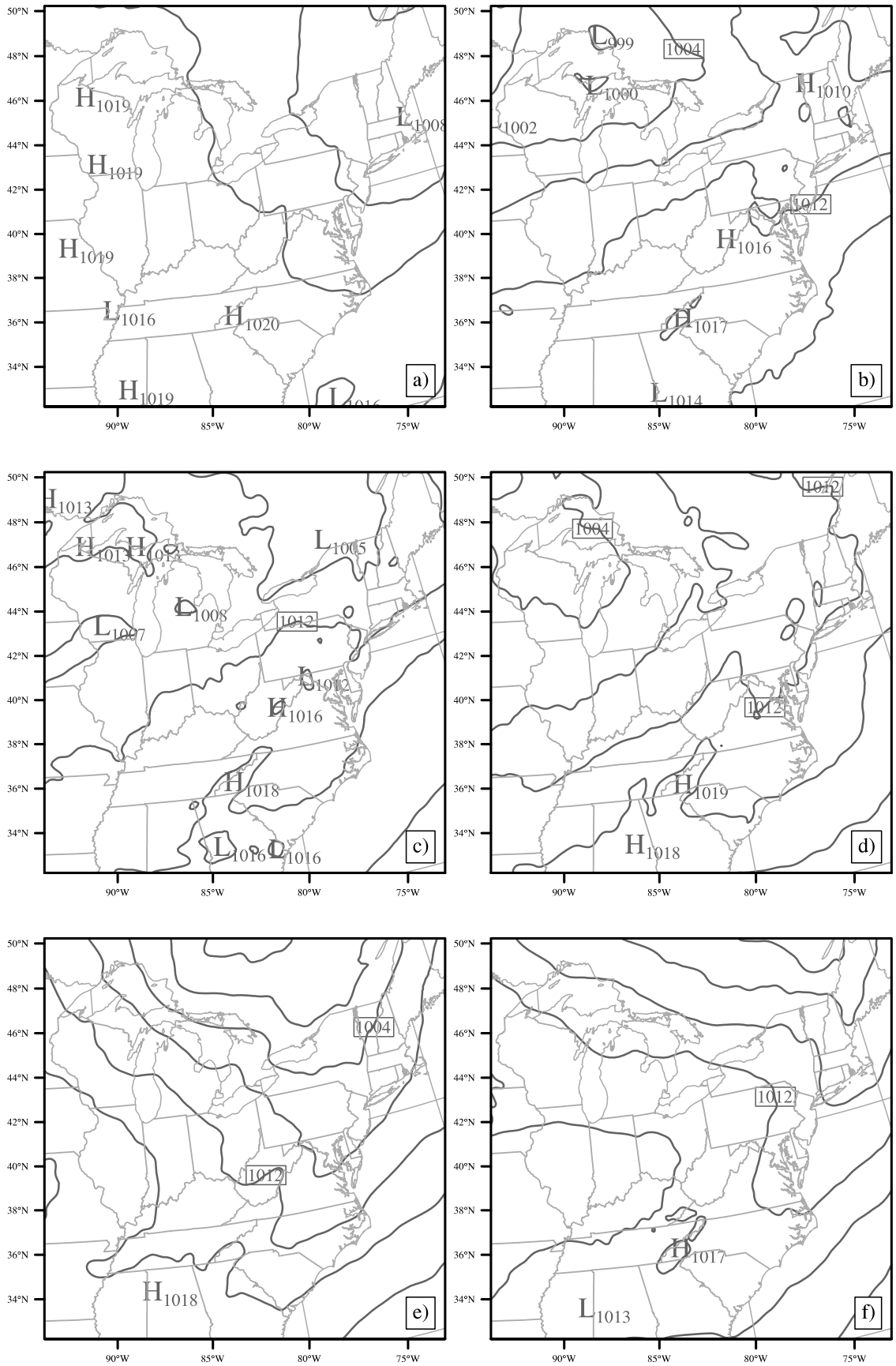
a)
b)
c)
d)
e)
f)
50°N
48°N
46°N
44°N
42°N
40°N
38°N
36°N
34°N
90°W
85°W
80°W
75°W
H1019
H1019
H1019
L1016
H1020
H1019
L1008
L999
1004
L1000
1002
H1010
1012
H1016
H1017
L1014
H1013
H1013
H1013
L1005
L1008
L1007
1012
L1012
H1016
H1018
L1016
L1016
1012
1004
1012
H1019
H1018
1004
1012
H1018
1012
H1017
L1013

Figure 2

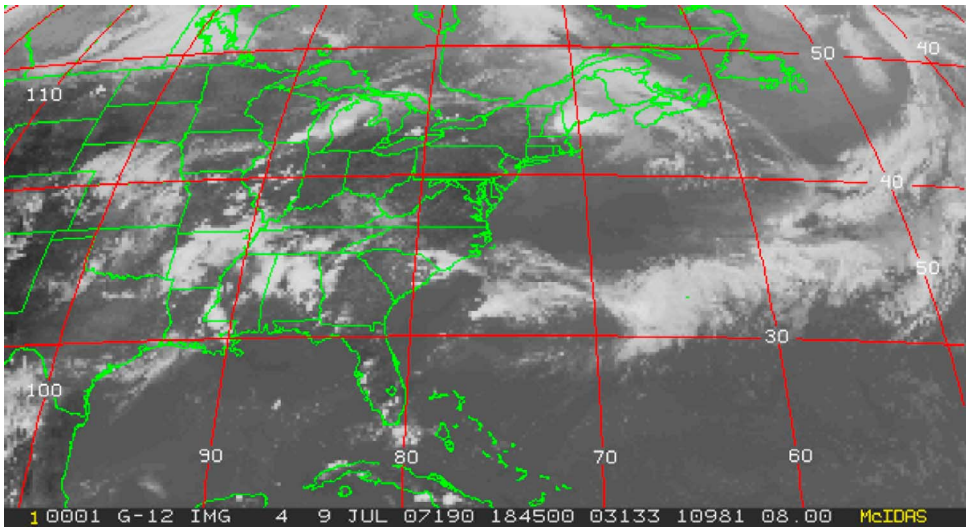

Figure 3. GOES-12 infrared image for 9 July 2007 18:45 UTC (13:45 LST). Note the cloud-free area associated with the high-pressure system over the eastern United States and area of deep convection stretching from Alabama to Georgia.

[22] Discrete forecasts were evaluated using mean bias, normalized mean bias (NMB), root mean square error (RMSE), normalized mean error (NME), correlation coefficient (r), and standard deviation (σ). Table 4 summarizes discrete observation-model O_3 comparisons. Average mean bias for the episode is 0.59 ppbv, with a standard deviation of ±11.0 ppbv; average NMB is 1.14%. The low mean bias is partially a result of overpredicted and underpredicted values in different regions of the domain canceling each other out as was shown in Tables 2 and 3. Mean biases on individual days are also small ranging from 2.9 ppbv on 6 July to −2.3 ppbv on 7 July. In terms of error, average WRF/Chem RMSE and NME values (11.0 ppbv and 16.2%) are on the lower end of previous studies (12–18 ppbv and 18–25%), respectively [e.g., *Kang and Elder*, 2005; *Eder et al.*, 2009; *Mao et al.*, 2010; *Zhang et al.*, 2006]. Low domain-wide biases often mask larger regional biases. For WRF/Chem O_3 low biases in the northeast United States exceeded 4 ppbv on 3 of 6 days and high biases in the southeast United States exceeded 6 ppbv on all 6 days. The correlation coefficient (r) between observations and model was approximately 0.7 for 7–10 July but was less than 0.5 on 6 and 11 July. Model performs the best on days when air quality is poor; on these days it simulates correctly the spatial pattern of surface O_3. In general, the model performance is comparable to NOAA's National Air Quality Forecast Capability (NAQFC) for July 2007, with slightly lower RMSE, NME and NMB [*Eder et al.*, 2009] (Table 4).

5.2.2. Categorical Statistics

[23] Categorical forecast evaluation was performed for the model nested domain using definitions of bias (B), false alarm ratio (FAR), critical success index (CSI) and hit rate (H) based on observed and modeled exceedances and nonexceedances. EPA's current National Ambient Air Quality Standard for 8 h maximum ozone of 75 ppbv was used as the threshold for exceedances. Variables (*a, b, c*, and *d*) used to calculate categorical metrics are defined as follows: *a* represents a forecast 8 h exceedance (>75 ppbv) that did not occur; *b*, a forecast 8 h exceedance that did occur; *c*, a forecast 8 h nonexceedance that did occur; and *d*, a nonforecast 8 h exceedance that did occur (Figure 6).

[24] Bias (B) is the measure of model's false negative and false positive forecasts. B < 1 indicates underprediction, B > 1 indicates overprediction, and B = 1 indicates no bias.

$$B = \left(\frac{a+b}{b+d}\right) \tag{5}$$

False alarm ratio (FAR) is the percentage of times an exceedance was forecast when none occurred.

$$FAR = \left(\frac{a}{a+b}\right) \cdot 100\% \tag{6}$$

Critical success index (CSI) measures how well forecasted and measured exceedances were predicted.

$$CSI = \left(\frac{b}{a+b+d}\right) \cdot 100\% \tag{7}$$

Figure 2. WRF/Chem sea level pressure (contoured by 4 hPa, black lines) on (a) 6 July 2007 12:00 UTC, (b) 8 July 2007 18:00 UTC, (c) 9 July 2007 18:00 UTC, (d) 10 July 2007 18:00 UTC, (e) 11 July 2007 18:00 UTC, and (f) 12 July 2007 03:00 UTC. The high-pressure system and approaching cold front are well simulated.

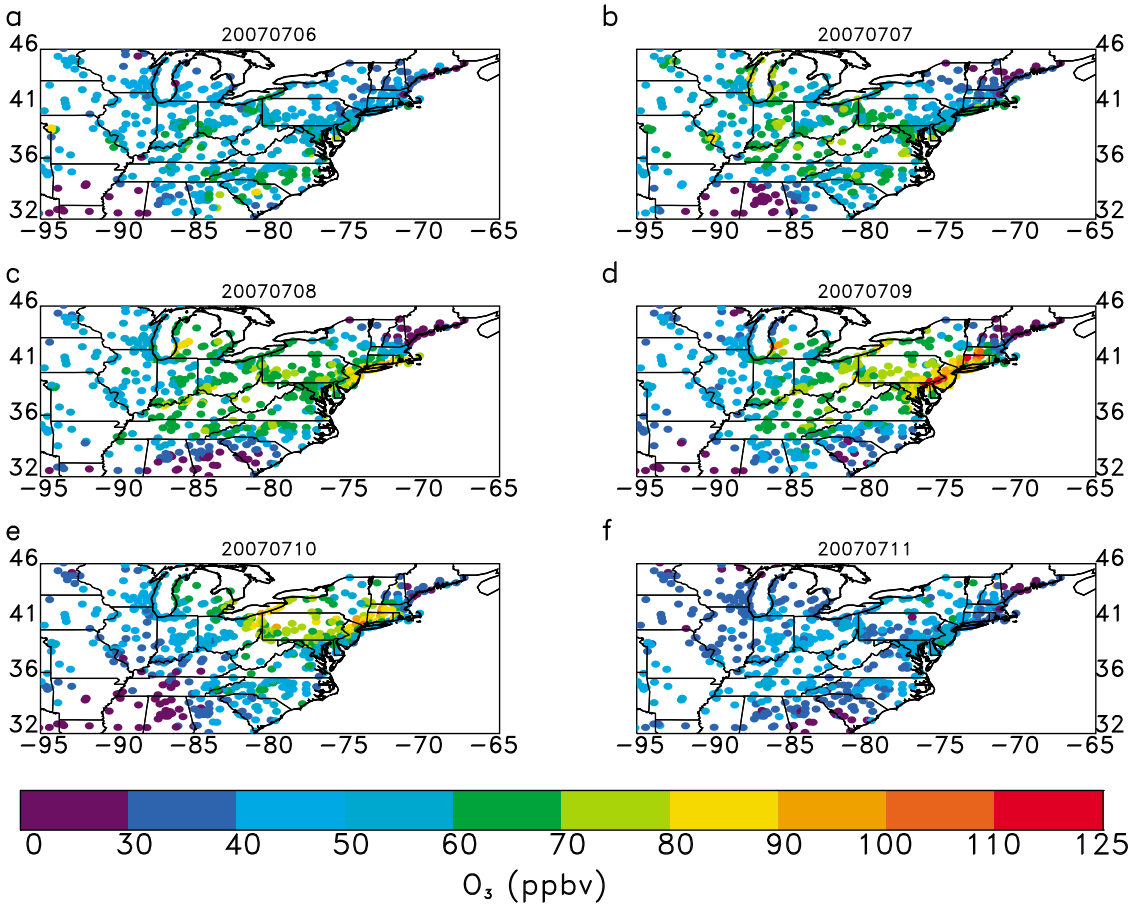

Figure 4. Observed surface 8 h O_3 daily maxima for (a) 6, (b) 7, (c) 8, (d) 9, (e) 10, and (f) 11 July 2007 with severe ozone event peaking on 9 July.

Last, the hit rate (H) is the percentage of observed exceedances that were forecasted.

$$H = \left(\frac{a}{b+d}\right) \cdot 100\% \tag{8}$$

Table 5 summarizes categorical evaluations for each day of the episode and for all data. On 6, 7 and 11 July, very few air quality violations were observed and the number of correctly forecast nonexceedances, is very large with respect to *a*, *b*, and *d*. Critical success index and hit rate measure model performance without consideration of correctly forecast observed nonexceedances. Overall, for this episode CSI is 30.6%; 9 July stands out with the highest CSI of 43.0%. Hit rate measures the percentage of correctly forecast observed exceedances. On 9 and 10 July the model has 48.6% and 44.6% hit rate. Bias indicates if forecast exceedances are underpredicted (B < 1) or overpredicted (B > 1). On all days the model's forecast exceedances are underpredicted, with the greatest bias on 10 July. Between 9 and 10 July, FAR values increased from 21.2% to 41.9%. The FAR was low on 9 July partially because modeled O_3 had a low bias in the northeast. The FAR increased on 10 July as the northeastern low bias disappeared and the resulting O_3 probability density function included more values in exceedance of 75 ppbv. Generally, WRF/Chem categorical statistics for the July smog event are comparable to NOAA's NAQFC model performance, with greater critical success index, and lower bias and false alarm ratio (Table 5).

6. Model-Observation Time Series Comparison

[25] In this section, 1 h daily measurements from stations in Maryland, New York, Tennessee and Georgia for 6–13 July 2007 are used to evaluate WRF/Chem.

6.1. Aldino, Maryland

[26] Time series of O_3 and NO_y ($NO_y = NO + NO_2 + PAN + HNO_3 + 2*N_2O_5 + HONO$ + organic nitrates) during 6–13 July 2007 at a suburban AQS station in Aldino, Maryland (downwind of Baltimore, Maryland), are shown in Figure 8. On the Aldino NO_y monitor the converter is located near the instrument inlet, so this represents a true NO_y measurement, without loss of HNO_3 as is typical of commercial compliance NO_x analyzers [e.g., *Poulida et al.*, 1994; *Schwab et al.*, 2009]. Observed and modeled O_3 mixing ratios showed an increasing trend in the daily maximum value from 6 through 9 July. On 9 July the observed O_3 concentration reaches a maximum of 139 ppbv around 14:00 LST, the model underpredicts this peak by 30 ppbv. The short-lived spike of 139 ppbv may be the result of the Chesapeake Bay breeze, a small-scale area of

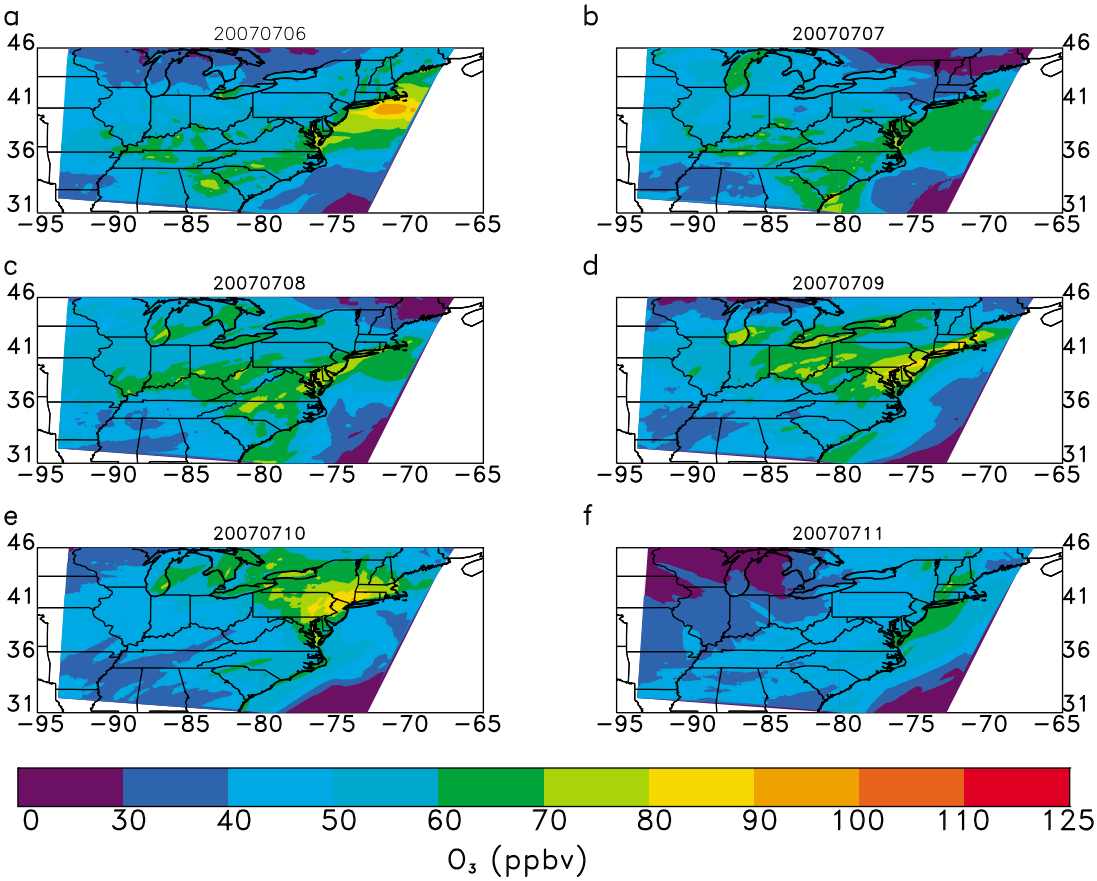

Figure 5. Modeled surface 8 h O_3 daily maxima for (a) 6, (b) 7, (c) 8, (d) 9, (e) 10, and (f) 11 July 2007. The severe smog event of 9–10 July is well simulated.

convergence formed along the northeast part of Washington, D. C., suburbs that is difficult to capture with the 12 km model resolution [*Loughner et al.*, 2011]. Overall, WRF/Chem captures the general shape of the diurnal cycle of ozone with minima in the early morning and maxima in the afternoon, with a daytime correlation coefficient (r) of 0.84 (Table 6, Aldino). Afternoon ozone maxima result from photochemical reactions of surface emitted CO, NO, and hydrocarbons [e.g., *Crutzen*, 1979]. Upper level transport of O_3 precursors from upwind emission sources and mixing into the planetary boundary layer also contributes to surface ozone maxima. At nighttime, photochemical production is suspended, and O_3 is lost by reaction with NO, VOCs and by dry deposition. Over the course of the smog event, WRF/Chem O_3 overestimates nighttime minima at Aldino by 7.26 ppbv (NMB = 21.9%); daytime maxima are underpredicted during the peak ozone days of 9–11 July. O_3 mean daytime bias is −5.97 ppbv (NMB = −10.0%) and mean daytime RMSE is 14.3 ppbv (NME = 17.4%) (Table 6, Aldino). The passage of a cold front seen in Figure 1f is evident in the decrease of observed and simulated O_3 at nighttime and early morning on 12 July.

Table 2. Daily Mean Bias (MB) for Observed and Simulated 8 h Maximum Ozone at AQS Sites for the Base WRF/Chem Simulation (E_BASE) and WRF/Chem With FDDA Nudging (E_FDDA)[a]

	MB (ppbv) (E_BASE)		MB (ppbv) (E_FDDA)	
	Northeast	Southeast	Northeast	Southeast
6 July 2007	1.14	6.86	0.19	9.26
7 July 2007	−4.62	10.5	−6.09	17.2
8 July 2007	−5.56	9.16	−3.43	19.6
9 July 2007	−6.93	6.30	−3.75	24.3
10 July 2007	0.13	7.28	11.0	21.4
11 July 2007	1.27	7.52	11.8	19.9
All	−2.43	7.94	1.62	20.5

[a]Bias calculated for two regions: northeast (Maryland, Delaware, Pennsylvania, New Jersey, and New York) and southeast (North Carolina, South Carolina, Georgia, Alabama, and Mississippi).

Table 3. Average Surface O_3 8 h Maximum Mean Bias (MB) Varying With Air Quality Monitored at AQS Sites for Base Case (E_BASE) and E_CHEM Simulations[a]

	MB Northeast (ppbv)			MB Southeast (ppbv)		
	E_BASE	E_CHEM	% Points	E_BASE	E_CHEM	% Points
O_3 < 40 ppbv	15.6	17.8	8%	14.5	16.8	45%
40–60 ppbv	3.68	6.1	42%	4.82	7.1	43%
O_3 > 60 ppbv	−7.76	−5.26	50%	−4.99	−3.22	11%

[a]E_CHEM simulations have N_2O_5 loss to aerosols turned off. Bias calculated for two regions: northeast (Maryland, Delaware, Pennsylvania, New Jersey, and New York) and southeast (North Carolina, South Carolina, Georgia, Alabama, and Mississippi). As was shown in Table 2, low model O_3 biases are seen for polluted conditions in the northeast United States, whereas high biases are seen for clean air conditions in the southeast United States.

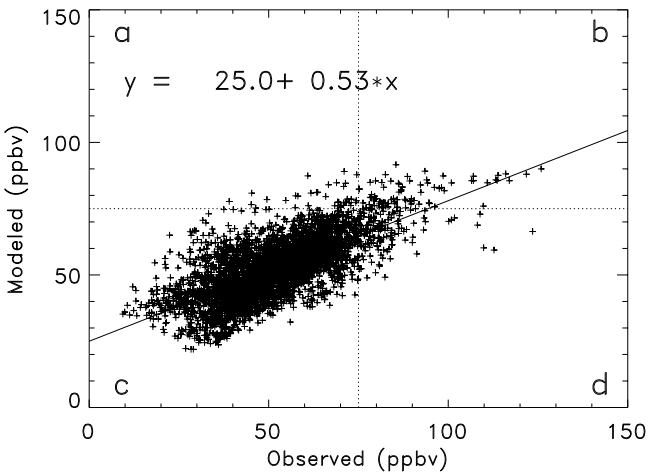

Figure 6. Scatterplot of the modeled versus observed 8 h maximum O_3 for 6–11 July 2007. Exceedance thresholds (75 ppbv), least squares regression line, and coefficients are shown. Means for model and observations are 54.7 ppbv and 54.2 ppbv, R = 0.7.

[27] Sensitivity simulation where O_3 dry deposition velocity in the model was doubled (E_DRYDEP) reduced nighttime O_3 by 11.4 ppbv changing the NMB from 21.9% to −12.1%. Daytime O_3 amounts decreased by 8.31 ppbv increasing the normalized low bias from 10% to 23% (Table 7). Clearly, O_3 amounts at Aldino are sensitive to dry deposition velocities and a low bias in V_d could be the cause of the nighttime high bias at Aldino. Other possible causes include an overestimation of vertical eddy diffusion (K_z too large) and/or an underestimation of titration (NO amounts too low due to excessive vertical mixing and/or a boundary layer that is too coarse to resolve nighttime chemistry).

[28] Total reactive nitrogen distributions are influenced by a combination of emission, photochemistry, and transport processes. The Aldino station is located in a suburban area, but in close proximity to I-95 interstate (~2 km). CO and NO_x emissions for the 12 km grid containing Aldino, are significantly influenced by interstate traffic. Observed NO_y reaches a maximum concentration in the early morning and a secondary maximum in the afternoon (Figure 8b). Vehicle emissions of NO_x contribute to the peaks during morning rush hour, especially on weekdays (9–11 July 2007). During the early afternoon, NO_y mixing ratios fall due to deepening of the planetary boundary layer (PBL), mixing, and loss by deposition. As the PBL height begins to decrease, NO_y mixing ratios increase in the late afternoon. In our evaluation of the Aldino, Maryland, site, WRF/Chem daytime NO_y normalized mean bias is 24.0% and NME is 54.7%. In the sensitivity simulation where NO_x conversion to nitric acid was suppressed (E_CHEM), model daytime O_3 and NO_y mean biases were reduced to −7.05% and 18.9%, respectively (Table 7, Day). This suburban site is sensitive to perturbations in ozone deposition velocity and the multiphase nitric acid formation reaction rate constant.

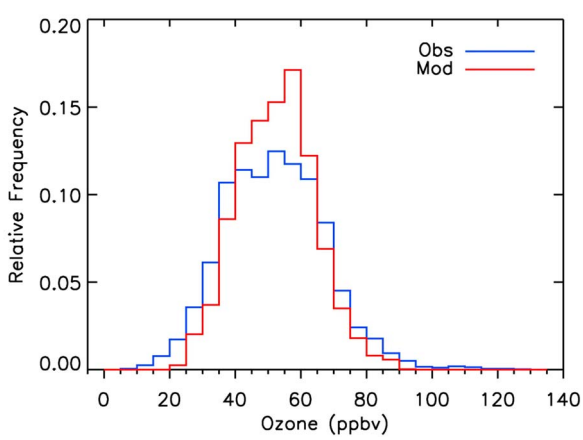

Figure 7. Frequency distribution of observed and modeled 8 h O_3 daily maxima for 6–11 July 2007. The model captures the mean but not the extremes of the distribution.

Table 4. Discrete Evaluation Results for Observed and Simulated 8 h Maximum Ozone at AQS Sites for Individual Days and All Days[a]

	MB (ppbv)	NMB (%)	RMSE (ppbv)	NME (%)	r	σ (ppbv)
6 July 2007	2.93	5.86	10.2	15.2	0.48	9.78
7 July 2007	−2.29	−4.22	10.2	14.9	0.69	9.94
8 July 2007	−0.86	−1.50	10.5	14.5	0.73	10.4
9 July 2007	0.23	0.38	13.1	16.9	0.74	13.1
10 July 2007	2.45	4.80	11.9	17.9	0.71	11.7
11 July 2007	1.06	2.57	9.75	18.6	0.37	9.70
All	0.59	1.14	11.0	16.2	0.70	11.0
NAQFC July 2007	5.50	11.9	12.7	20.9	0.70	

[a]July 2007 NAQFC (WRF-CMAQ) performance from *Eder et al.* [2009] is also shown for comparison. MB, mean bias; NMB, normalized mean bias; RMSE, root-mean-square error; NME, normalized mean error; r, correlation coefficient; σ, standard deviation.

6.2. Pinnacle State Park, New York

[29] Observations of trace species and meteorological variables at Pinnacle State Park research site (elev. 504 m above sea level) are shown in Figure 9. At this remote site, trace gas measurements are available only for the beginning and end of the simulated period due to failure of air conditioning in the instrument shelter. Model O_3 tracks the diurnal variation seen in observations (r = 0.86). The model underpredicts O_3 at this site, NMB and RMSE for O_3 are −14.3% and 9.20 ppbv. Similarly to the Aldino, Maryland, site, the cold front marched through at nighttime on 11–

Table 5. Categorical Evaluation Results for Observed and Simulated 8 h Maximum Ozone at AQS Sites[a]

	B	FAR (%)	CSI (%)	H (%)	*a*	*b*	*c*	*d*
6 July 2007	0.67	100	0	0	2	0	594	3
7 July 2007	0	N/A	0	0	0	0	580	16
8 July 2007	0.11	20	8.30	8.50	1	4	548	43
9 July 2007	0.62	21.2	43.0	48.6	14	52	480	55
10 July 2007	0.77	41.9	33.8	44.6	18	25	527	31
11 July 2007	0	N/A	0	0	0	0	599	1
All	0.50	30.2	30.6	35.2	35	81	3328	149
NAQFC July 2007	1.90	80.9	14.2	35.5				

[a]Results for 6, 7, and 11 July are not statistically significant, since *a* and *b* ≈ 0. July 2007 NAQFC (WRF-CMAQ) performance from *Eder et al.* [2009] is also shown for comparison. B, bias; FAR, false alarm ratio; CSI, critical success index; H, hit rate.

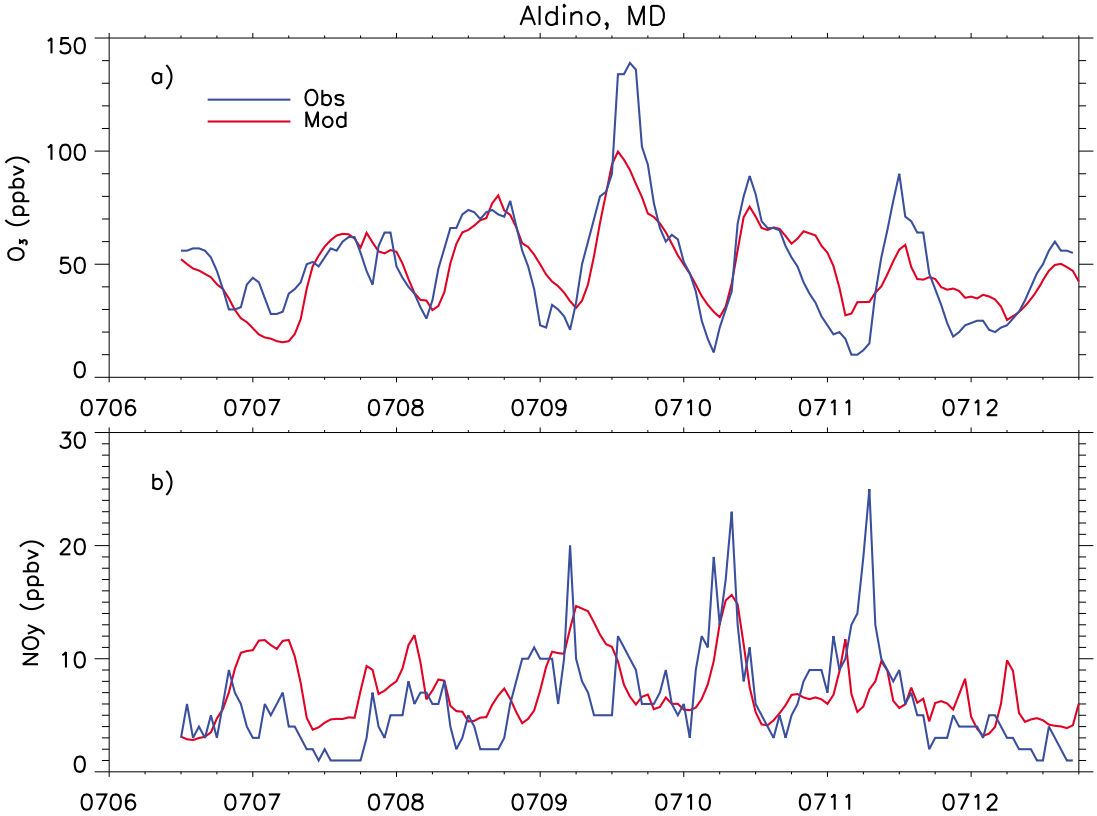

Figure 8. Time series of observed (blue line) and simulated (red line) 1 h (a) O_3 and (b) NO_y daily maxima at urban Aldino, Maryland, AQS site for 6–13 July 2007 (LST). The model reproduces the observed concentrations, except the ozone maximum on 9 July, which may be due to subgrid-scale bay breeze [*Loughner et al.*, 2011].

12 July as seen in hourly O_3 and temperature measurements (Figures 9a and 9c).

[30] CO is a good tracer for transport due to its long lifetime of approximately a month. Predicted daytime CO is generally in good agreement with the observations (NMB: 8.42%, NME: 14.6%) indicating that transport from upwind sources is sufficiently well represented by the model. The model has the drop in CO due to cold front passage a little early, but overpredicts slightly at other times. Basic diurnal cycles of air temperature (Figure 9c) are represented by the model with correlation coefficient r = 0.87. WRF/Chem air temperature is overpredicted by 1.42°C at night and underpredicted by 0.35°C during the day. NO_y, NO_x, and NO_z ($NO_y - NO_x$) measurements are below 8 ppbv (Figures 9d–9f) characteristic of a rural location, with occasional perturbations by local vehicle emissions. The model underestimates daytime NO_y by 5.01% and overestimates NO_x by 3.44% (Table 7); these are small model/measurement differences. When N_2O_5 loss was turned off, daytime NO_x went from underestimated by 5% to overestimated by 3%, a relatively minor change. The mean bias in daytime ozone improved slightly from −14% to −10%, indicating that ozone formation is somewhat sensitive to NO_x concentrations at this rural site. Examination of the model fields indicates that HNO_3 is the primary NO_z/NO_y component on the afternoon of 10 July when the model shows a large high bias.

[31] In summary, daytime and nighttime normalized mean biases of O_3 and NO_y were reduced in the E_CHEM simulation (Table 7), which provides an upper limit on NO_x recycling at this site. Similar to the Aldino site, prediction of O_3 was improved by extending the lifetime of NO_x and its availability for O_3 formation.

6.3. Great Smoky Mountains, Tennessee

[32] Measurements of O_3, CO, NO_x and air temperature at Great Smoky Mountains site (elev. 793 m above sea level) are shown in Figure 10; the model is too clean and too cool. At this site the model does not exhibit observed diurnal variation of ozone, with poor daytime correlation (r = 0.47). Daytime ozone normalized mean bias and normalized error are −13.4% and 23.9%, respectively. Observed CO amounts and diurnal variations are underestimated substantially by the model. Similar to the Pinnacle site, at this mountain site, our 12 km nested WRF/Chem simulation is not expected to capture the small-scale processes associated with orography. On average, the model overpredicts daytime and nighttime air temperature by 2.25°C and 2.04°C, respectively.

[33] WRF/Chem underestimates NO_x at this site, with daytime and nighttime NMB of −36.3% and −13.2%. WRF/Chem shows simultaneous low bias in NO_x mixing ratios and low bias in surface O_3. The results are sensitive to the rate at which N_2O_5 is converted to HNO_3. In E_CHEM

Table 6. WRF/Chem (E_BASE) Discrete Evaluation for Individual Observation Sites Calculated for Daytime Hours on 6–12 July[a]

	$\overline{Obs}$ (ppbv)	MB (ppbv)	NMB (%)	RMSE (ppbv)	NME (%)	r	SD (ppbv)
			Aldino				
O_3	59.6	−5.97	−10.0	14.3	17.4	0.84	13.1
NO_y	5.55	1.32	24.0	4.08	54.7	0.53	3.88
			Pinnacle				
O_3	53.0	−7.33	−14.3	9.2	16.1	0.86	6.58
CO	−147.5	12.0	8.42	24.2	14.6	0.3	23.4
NO_y	3.05	−0.15	−5.01	0.88	24.7	0.74	0.92
NO_x	1.06	0.03	3.44	0.71	52.5	0.12	0.78
NO_z	1.98	−0.16	−8.57	0.47	21.4	0.83	0.49
Temp	24.9	0.35	1.45	2.19	6.2	0.87	2.17
			Smokies				
O_3	51.0	−6.82	−13.4	15.4	23.9	0.47	13.9
CO	163.8	−17.5	−10.7	54.4	25.4	−0.08	51.8
NO_x	2.18	−0.79	−36.3	1.32	49.2	0.44	1.07
Temp	22.5	2.25	10.0	3.61	13.6	0.36	2.83
			SEARCH–JST				
O_3	32.5	0.89	2.7	16.0	37.4	0.52	16.1
CO	214.4	200.4	93.6	310.3	101.4	0.15	253.7
NO_y	14.1	9.67	68.8	19.0	91.0	0.31	16.6
NO_x	12.6	8.82	70.6	18.9	101.2	0.27	16.9
NO_z	1.73	0.63	36.0	1.65	78.4	0.48	1.55
Temp	26.6	1.48	5.56	4.14	12.0	0.18	3.89
			SEARCH–YRK				
O_3	11.0	4.48	12.4	8.73	26.6	0.55	11.3
CO	277.3	7.17	5.04	39.9	20.8	0.36	41.0
NO_y	24.9	1.97	70.2	3.07	81.2	0.27	2.36
NO_x	24.4	1.21	62.6	2.34	89.8	0.3	2.01
NO_z	0.51	0.76	86.9	1.05	95.2	0.47	0.73
Temp	22.5	1.8	7.35	4.78	14.6	−0.01	4.46

[a]Daytime hours are 06:00–20:00 LST. $\overline{Obs}$, observations; MB, mean bias; NMB, normalized mean bias; RMSE, root-mean-square error; NME, normalized mean error; r, correlation coefficient; SD, standard deviation.

sensitivity simulation where the N_2O_5 conversion to HNO_3 was set to zero, daytime O_3 mean bias was reduced from −13.4% to −7.61% while NO_x low mean bias increased from 36.3% to 47.7% (Table 7). As at Aldino and Pinnacles sites, increased NO_x recycling reduced the magnitude of daytime and nighttime O_3 biases.

6.4. SEARCH Sites, Georgia

[34] Figure 11 compares observed and modeled trace gas species and meteorological variables at an urban SEARCH Jefferson St site (JST) in Atlanta, Georgia. Observations and the model exhibit the daytime peaks and nighttime troughs associated with ozone production during the day and destruction at night. CO normalized mean bias at this site is 93.6% and correlation coefficient (r) is 0.15 (Table 6, SEARCH–JST). Observed CO mixing ratios (<400 ppbv) are lower than what is typically observed in an urban region such as downtown Atlanta, Georgia (600–800 ppbv) [*Blanchard and Tanenbaum*, 2006]. Observed CO to NO_x ratios are also much lower than EPA published 10:1 ratio for

Table 7. WRF/Chem E_BASE, E_CHEM, and E_DRYDEP Mean Daytime and Nighttime O_3, NO_y, and NO_x Biases for Observation Sites[a]

	NMB O_3 (%)			NMB NO_y (%)			NMB NO_x (%)		
	E_BASE	E_CHEM	E_DRYDEP	E_BASE	E_CHEM	E_DRYDEP	E_BASE	E_CHEM NMB	E_DRYDEP
					Day				
Aldino	−10.0	−7.05	−23.1	24.0	18.9	17.9	N/A	N/A	N/A
Pinnacles	−14.3	−9.89	−30.2	−5.01	3.12	−1.18	3.44	13.0	9.42
Smokies	−13.4	−7.61	−23.9	N/A	N/A	N/A	−36.3	−47.7	−48.7
JST	2.7	15.1	−0.98	68.8	75.8	75.3	70.6	74.8	74.9
YRK	12.4	31.0	10.6	70.2	67.7	65.3	62.6	54.8	54.0
					Night				
Aldino	21.9	25.2	−12.1	4.26	6.16	6.22	N/A	N/A	N/A
Pinnacles	−18.0	−16.3	−37.3	−13.2	−8.67	−10.8	−32.0	−17.9	−21.1
Smokies	−20.1	−15.0	−35.6	N/A	N/A	N/A	−13.2	−16.5	−15.4
JST	39.4	43.6	−10.0	1.78	4.26	4.51	−1.68	1.07	1.32
YRK	16.4	24.0	−7.74	11.3	13.8	14.8	−4.82	−2.06	−0.71

[a]E_CHEM simulations have N_2O_5 loss to aerosols turned off. NMB, normalized mean bias.

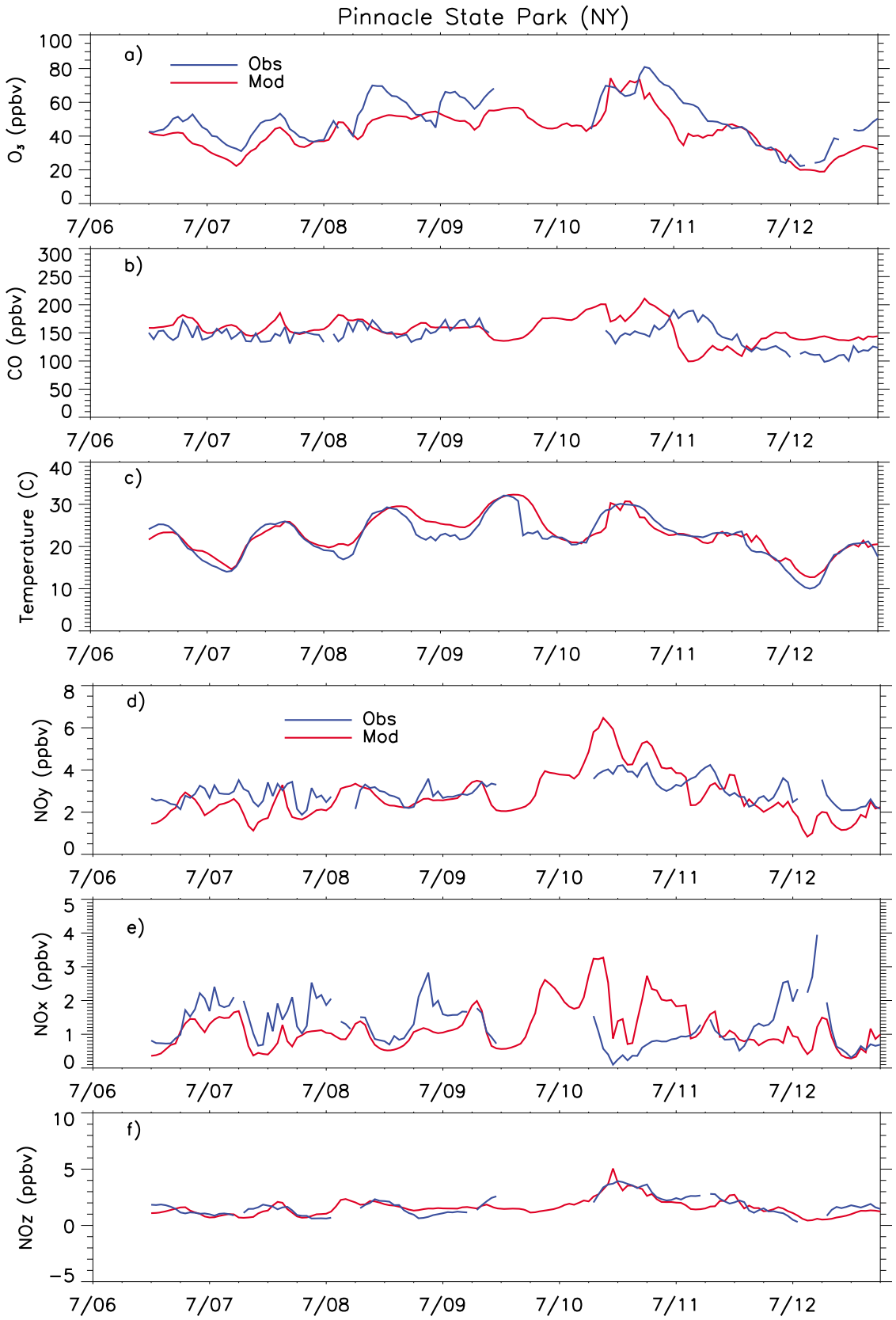
Pinnacle State Park (NY)
a)
Obs
Mod
O3 (ppbv)
b)
CO (ppbv)
c)
Temperature (C)
d)
Obs
Mod
NOy (ppbv)
e)
NOx (ppbv)
f)
NOz (ppbv)
7/06
7/07
7/08
7/09
7/10
7/11
7/12

Figure 9

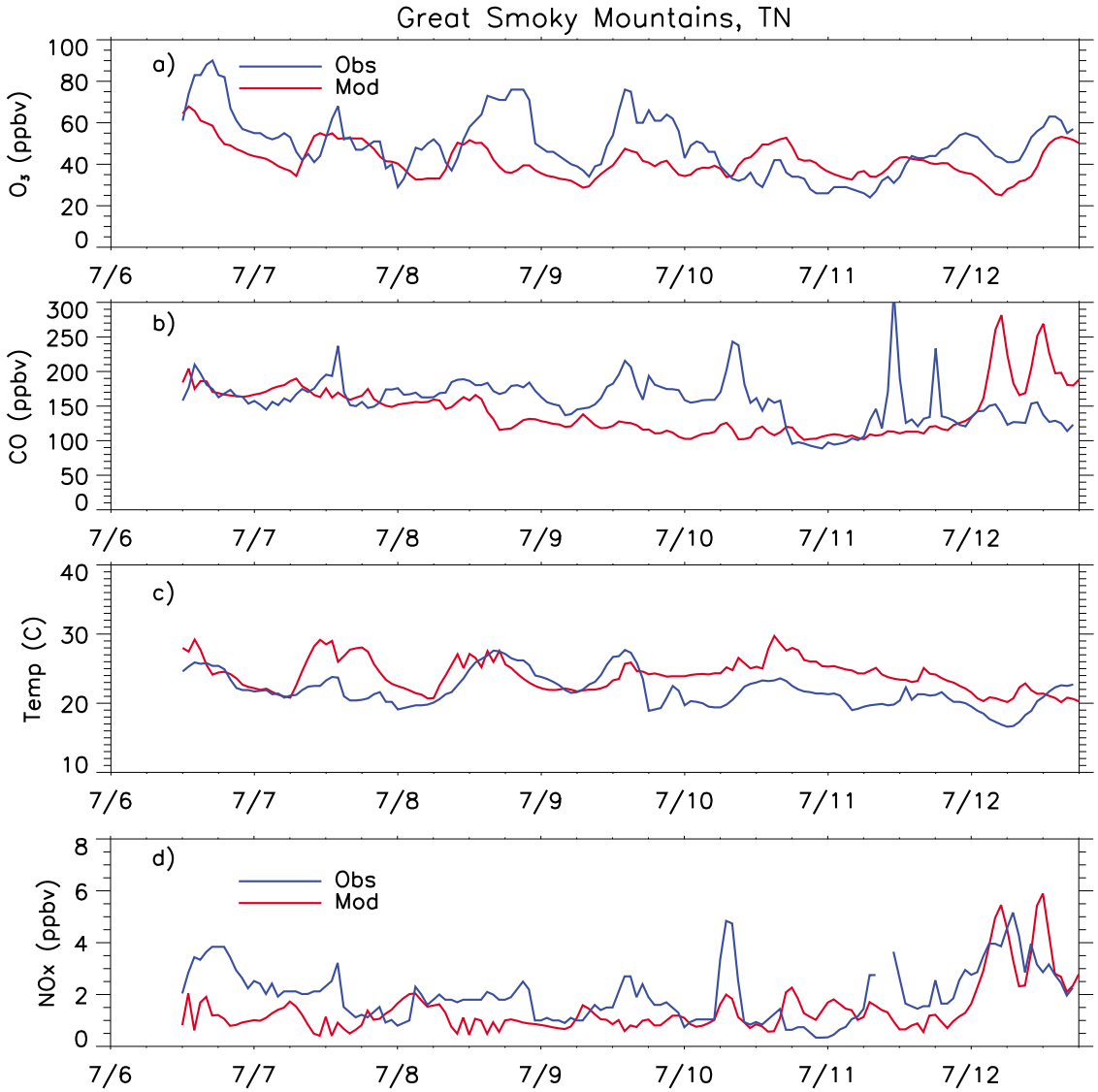

Figure 10. Time series of observed (blue line) and simulated (red line) 1 h daily maxima at Great Smoky Mountains, TN site for July 6–13, 2007 (LST):): (a) O_3, (b) CO, (c) temperature, and (d) NO_y. On average the model underestimates pollutant concentrations. Minimizing the NO_x loss via heterogeneous processes and accounting for NO_x recycling through $ClNO_2$ can improve the bias in ozone; see text.

an area where a combination of gasoline and diesel fueled vehicles is present (available at http://www.epa.gov/ttn/chief/trends/). These inconsistencies could indicate a problem with the CO measurements. Alternatively, the poor agreement with observations could indicate that CO motor vehicle emissions (MOBILE6) used in this study are overestimated. *Parrish* [2006] showed that CO emissions from motor vehicles in MOBILE6 are overestimated by a factor of 2 in comparison with a fuel-based inventory. Moreover, *Kuhns et al.* [2004] compared MOBILE6 CO emission factors to those measured by vehicle exhaust remote sensing; MOBILE6 CO emission factors were 2 times greater than measured CO emission factors for vehicles less than 13 years old. According to the EPA 2002 national inventory within Fulton County (metropolitan Atlanta), on-highway and off-highway motor vehicles accounted for 98% of CO emissions and 87% of NO_x emissions [available at http://www.epa.gov/air/data]. By contrast, in northeastern U.S.

Figure 9. Time series of observed (blue line) and simulated (red line) 1 h daily maxima at Pinnacle State Park, New York, site for 6–13 July 2007 (LST): (a) O_3, (b) CO, (c) temperature, (d) NO_y, (e) NO_x, and (f) NO_z. Missing data on 9–10 July due to failure of air conditioning in the instrument shelter. The base run of the model tends to underestimate O_3 and NO_x, its principal precursor. Minimizing the NO_x loss due to heterogeneous reactions and accounting for NO_x recycling through $ClNO_2$ can improve these biases; see text.

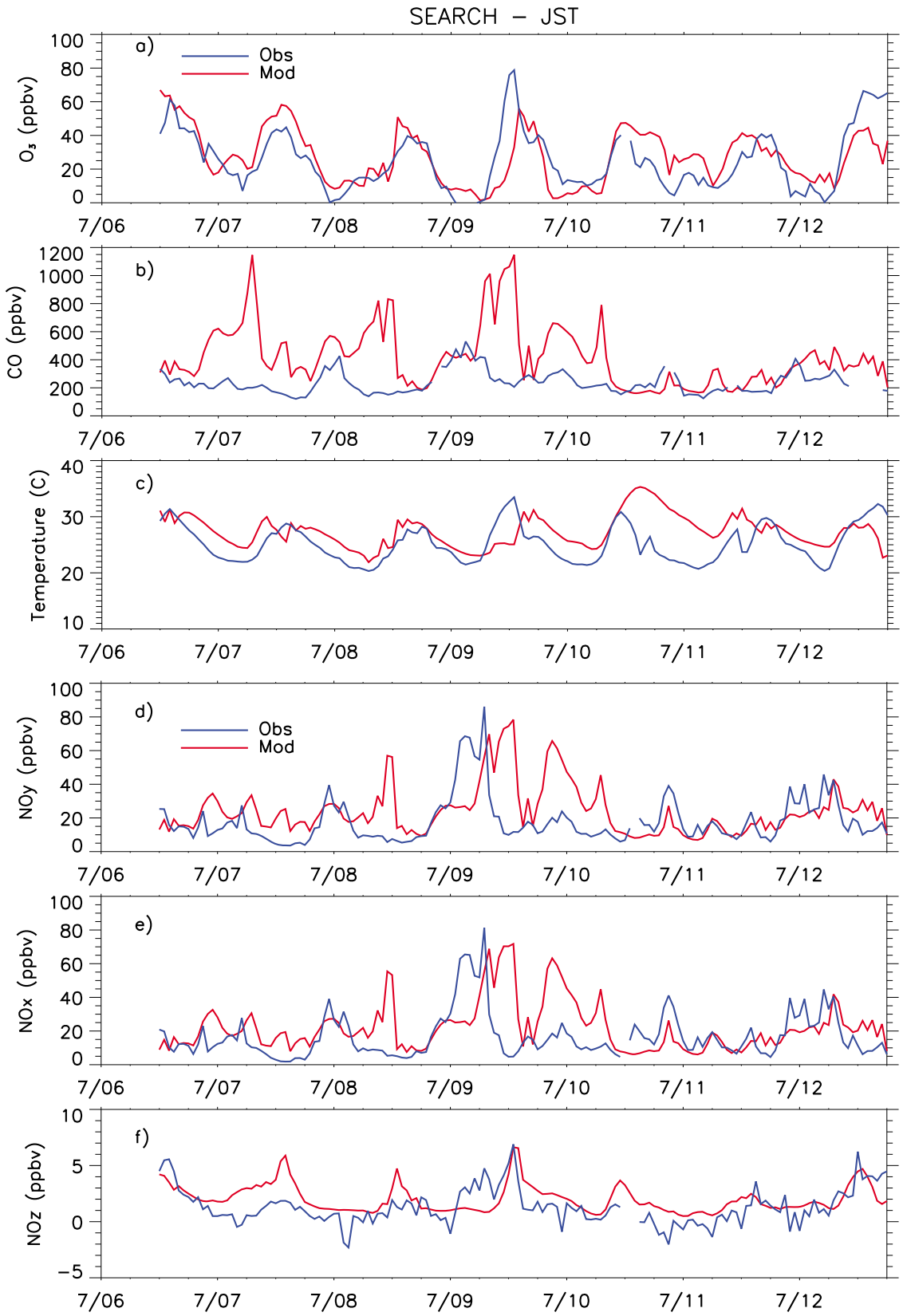

Figure 11. Time series of observed (blue line) and simulated (red line) 1 h daily maxima at SEARCH–JST, Georgia, site for 6–13 July 2007 (LST): (a) O_3, (b) CO, (c) temperature, (d) NO_y, (e) NO_x, and (f) NO_z. The model overestimates ozone and temperature but does on average reasonably well with NO_x. Doubling the ozone dry deposition velocity improves model measurement agreement as discussed in the text.

on-highway and off-highway motor vehicles account for 91% of CO emissions and only 58% of NO_x emissions. Therefore, higher accuracy in model representation of CO and NO_x emissions from mobile sources is especially important in the southeast United States.

[35] The model does a reasonable job with daytime ozone maxima, but underestimates peak O_3 on 9 July. WRF/Chem daytime ozone mean bias is 0.89 ppbv (NMB of 2.70%) and RMSE of 16.0 ppbv (NME of 37.4%), while correlation coefficient is moderate (r = 0.52). Nighttime O_3 mixing ratios below 10 ppbv were observed during most of the comparison period. Single digit O_3 mixing ratios at nighttime are attributed to nighttime depletion of surface O_3 by dry deposition and titration with limited resupply of O_3-rich air from aloft [*Talbot et al.*, 2005]. Nighttime ozone destruction in the model is not as efficient possibly due to an underestimation of O_3 dry deposition. In E_DRYDEP simulation daytime (nighttime) O_3 normalized mean bias was reduced from 2.7 (39.4)% to −0.98 (−10.0)% when the deposition velocity was doubled. Of course, biases in nighttime O_3 can also arise from overpredicted vertical mixing, and consequently underpredicted nighttime titration of O_3 by reaction with NO, and/or coarse model resolution of the first model layer.

[36] Figures 11d–11f compare observed and simulated NO_y, NO_x and NO_z species at JST. WRF/Chem overpredicts daytime NO_y, NO_x and NO_z peaks with normalized mean biases of 68.8%, 70.6% and 36.0%, respectively. The timing of modeled and observed peaks in NO_y, NO_x, and O_3 on 9 July appear to be controlled by the timing of convection. Observed concentrations rise rapidly in the morning but decrease sharply around 13:00 local time when thunderstorms rolled through the area. Modeled concentrations rise slower (never reaching observed peaks) but for a longer period of time as the modeled convection occurs at least 2 h after the observed event. When the storms arrive, polluted boundary layer air is mixed with cleaner upper level air, decreasing surface mixing ratios of O_3, CO, and nitrogen species (Figure 3). Figure 12 compares measurements and simulation results at a rural SEARCH Yorkville, Georgia, site. Available ozone measurements during the 9–12 July 2007 period show model daytime and nighttime overestimation with NMB of 12.4% and 16.4%, respectively. This may result from excess import of O_3 or the nighttime mean bias in temperature of 2.46°C. Warmer nighttime surface temperatures are characteristic of deeper nocturnal boundary layer, lower surface NO_x concentrations due to vertical redistribution and less titration of O_3 by NO. At YRK, CO has no significant diurnal pattern, indicative of the rural nature of this site distant from mobile source emissions. NO_y, NO_x and NO_z daytime normalized mean bias is 70.2%, 62.6% and 86.9%, respectively. Similarly to JST site, increased O_3 dry deposition at this site improves both daytime and modeled performance (Table 7). E_CHEM sensitivity simulation decreased biases in daytime and nighttime NO_x at YRK site, but this contributed to significant overproduction of O_3.

[37] In summary, WRF/Chem captures the diurnal variability of O_3 and NO_y species at Aldino, Pinnacles, Great Smokies and SEARCH sites over the course of the smog episode, terminated by the timely passage of the cold front in the model. Sensitivity simulations increasing O_3 dry deposition decreased nighttime O_3 biases at Aldino and SEARCH sites. Additional sensitivity simulations that minimized NO_x loss via heterogeneous processes and maximized NO_x recycling through $ClNO_2$ chemistry improved model performance in the polluted northeast, especially the remote Pinnacles site, but increased model bias in the moderately polluted southeast (Table 3), resulting in MB of 3.99 ppbv, RMSE of 11.92 and R = 0.7. In general, the model is more sensitive to changes in meteorological fields (i.e., temperature) than chemical factors (i.e., dry deposition velocity and N_2O_5 reaction rate coefficient). A FDDA sensitivity run increased temperature bias at southeast U.S. sites, increasing O_3 MB in southeast United States by 12 ppbv. Where the model succeeds at predicting temperature and NO_x concentrations the calculated O_3 fields agree best with observations. There remains much more to learn about the causes of biases between modeled and measured ozone in the southeast United States.

7. WRF/Chem Vertical Analysis

[38] Figure 13 shows WRF/Chem simulated O_3 on 6 layers: surface, 950 hPa, 910 hPa, 815 hPa, 730 hPa, and 685 hPa for 18:00 UTC 9 July 2007. The signature of the smog event in northeast United States is most visible from the surface to 815 hPa. Pollutant outflow into the Atlantic from densely populated metropolitan areas along I-95 corridor is greatest in the 950 hPa and 910 hPa layers. Enhanced ozone above 730 hPa is associated with upper level regional transport of ozone and its precursors driven by midlatitude cyclonic wind patterns.

[39] Several ozonesondes were launched during the 6–11 July 2007 ozone episode at Beltsville, Maryland (76.5°W, 39.0°N) [*Yorks et al.*, 2009]. Ozonesonde launches took place in a wooded area 19 km northeast of Washington, D. C., under the auspices of Howard University and NASA's Goddard Space Flight Center. Profiles from WRF/Chem experiments are compared to afternoon and nighttime ozonesonde profiles (Figure 14). On 9 July at 18:00 UTC, a 100–113 ppbv layer of ozone is observed from surface to 800 hPa (Figure 14a). WRF/Chem matches the shape of the ozonesonde profile up to 650 hPa, but the magnitude is low by 13–25 ppbv below 800 hPa, as was seen in comparison to surface observations (Figures 4d and 5d). Between 600 and 250 hPa, WRF/Chem overestimates ozone by as much as 28 ppbv. Inclusion of MOZART-4 chemical initial and boundary conditions and the coarse vertical model resolution in the mid to upper troposphere exacerbates the WRF/Chem bias. More than 90% of the model bias above 450 hPa is due to MOZART-4 O_3 contribution. Our findings agree with previous work by *Yu et al.* [2007], who reported overestimation of O_3 above 6 km due to lateral boundary conditions. They noted that the boundary condition induced biases would likely decrease if the vertical resolution of the regional model was increased. Observed and predicted relative humidity increase with altitude from 30% at the surface to 70% at 800 hPa (Figure 14b). The model relative humidity continues to increase from 800 hPa to 750 hPa reaching 100% at 750 hPa before sharply decreasing to 20% at 610 hPa. This suggests that the model mixing height is overpredicted by

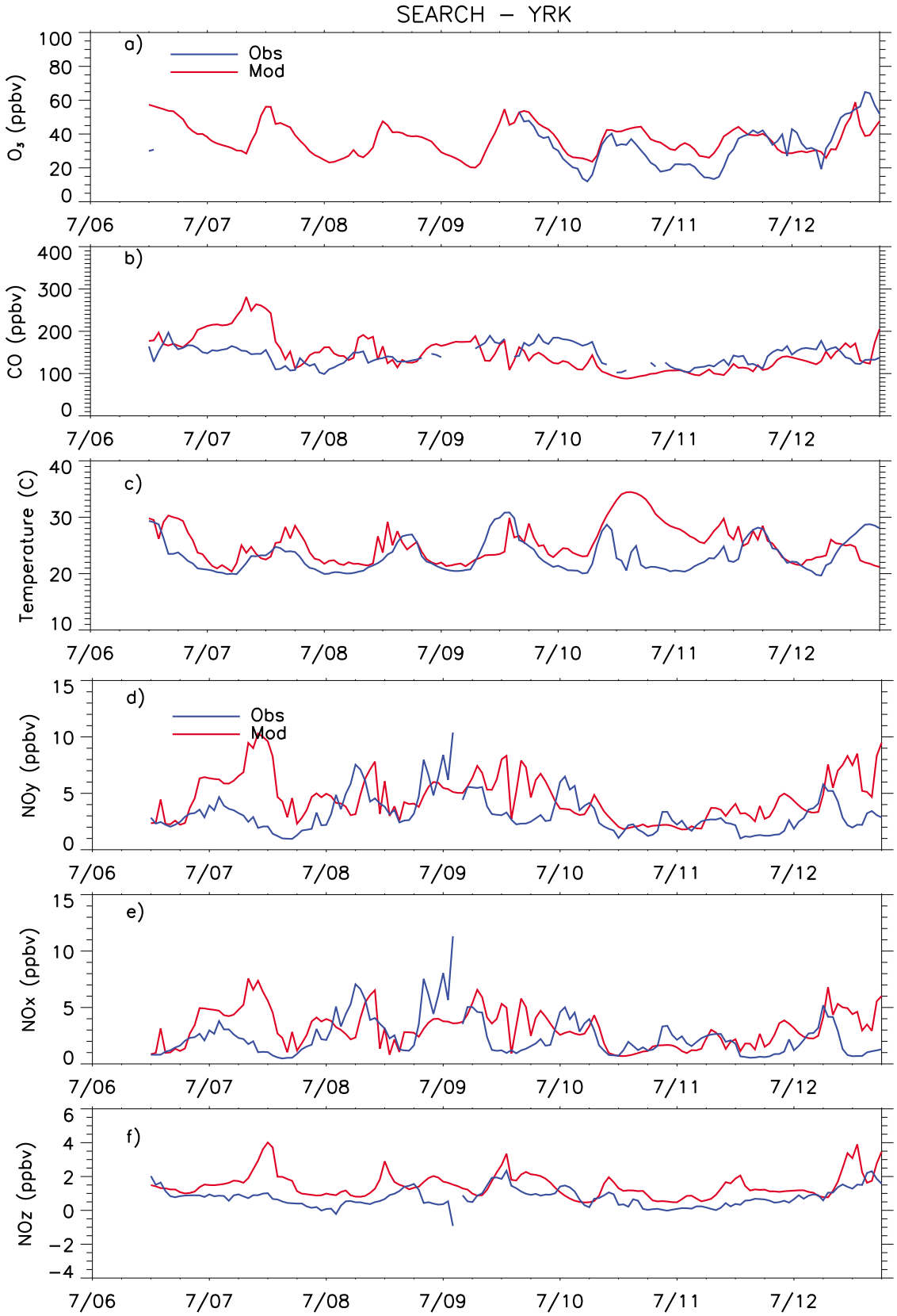

Figure 12. Time series of observed (blue line) and simulated (red line) 1 h O_3 daily maxima at the rural SEARCH–YRK, Georgia, site for 6–13 July 2007 (LST): (a) O_3, (b) CO, (c) temperature, (d) NO_y, (e) NO_x, and (f) NO_z. The model overestimates ozone and temperature, but does on average reasonably with NO_x.

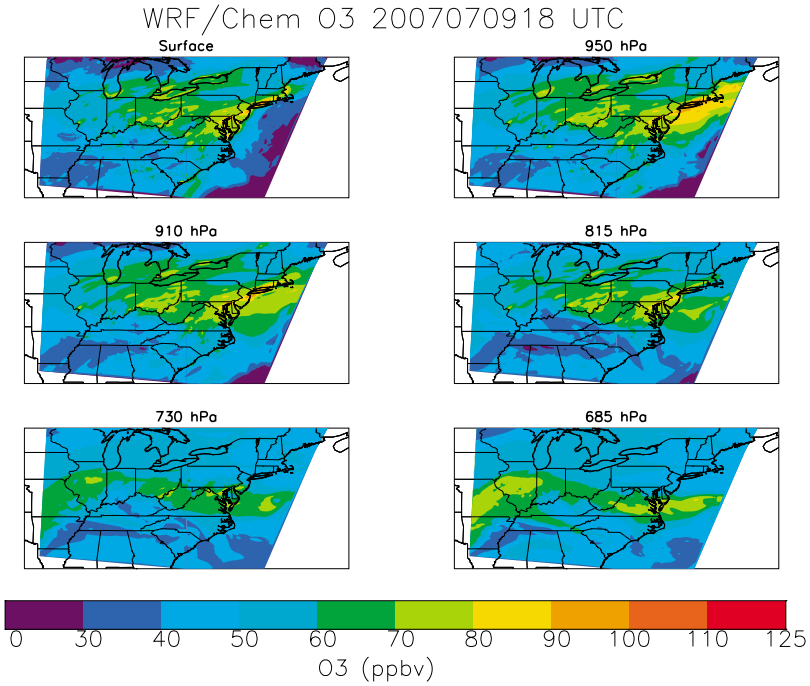

Figure 13. WRF/Chem O_3 at the surface, 950 hPa, 910 hPa, 815 hPa, 730 hPa, and 685 hPa for 18:00 UTC (13:00 LST) 9 July 2007. Even in the afternoon, the maximum ozone is seen a few 100 m above the surface at 910–950 hPa.

approximately 50 hPa (or 500 m), consistent with the model O_3 profile. Underprediction of surface O_3 at this site is likely partially due to overprediction of the planetary boundary layer height. In the mid to upper troposphere, observed and modeled relative humidity is on average below 30%, suggesting subsidence and an upper tropospheric origin (Figure 14b).

[40] Another sounding was launched 12 h later at 06:00 UTC on 10 July (Figure 14c). In this ozone sounding there is a local minimum at about 960 hPa. The vertical scale of this inversion is too small to be resolved by the model simulation. Observed and modeled ozone mixing ratios in the boundary layer drop below 45 ppbv as ozone is removed by dry deposition and chemical titration. At nighttime, observed ozone in the 960 to 800 hPa layer decreased to 65 ppbv, although above 800 hPa the profile is similar to the 18:00 UTC sounding up to 350 hPa. The model overpredicts nighttime PBL and midtropospheric ozone by 10–20 ppbv, with highest biases at 400 hPa. The overprediction in nighttime O_3 may be caused by overestimation of vertical mixing (K_z too large) as shown by *Castellanos et al.* [2011]. Observed and modeled relative humidity is enhanced around 800 hPa and 280 hPa. The model does not capture the peak in relative humidity seen at 600 hPa or the minimum between 700 and 800 hPa. In comparison with daytime observations, both the model and observations (Figure 14d) show enhanced relative humidity (65–75%) in the 340 hPa to 270 hPa levels; modeled and observed O_3 are enhanced 15 and 25 ppbv, respectively. Ozone production halts at night within the PBL, regional advective redistribution of ozone enhances mixing ratios at upper levels (above 350 hPa), while accumulated ozone in the mid troposphere (600–350 hPa) is greater than on previous day. Overall, model measurement agreement for ozone is good given the resolution of the model.

[41] In the afternoon sounding on 10 July 20:00 UTC (Figure 14e), surface ozone is just 50 ppbv increasing with altitude to 95 ppbv at 830 hPa. Above the planetary boundary layer, ozone increases gradually with height reaching 110–120 ppbv in the 400–280 hPa layer. O_3 increase between 400 and 280 hPa is associated with transport from upwind lightning activity accompanied by photochemical ozone production [*Dickerson et al.*, 1987; *Pickering et al.*, 1992]. On 9 July 2007 at 18:00 UTC, there was significant thunderstorm activity across Alabama and Mississippi according to the NCDC radar reflectivity archive. GOES-12 IR infrared shows the spatial extent of this storm (Figure 3). HYSPLIT (R. R. Draxler and G. D. Rolph, HYSPLIT (HYbrid Single-Particle Lagrangian Integrated Trajectory) Model, 2003, http://www.arl.noaa.gov/ready/hysplit4.html) back trajectory started on 10 July 20:00 UTC at 400 hPa at Beltsville, Maryland, confirm passage of the sampled air mass through Alabama and Mississippi convective storms. Figure 15 shows MODIS cloud top pressure during the 9 July 18:00 UTC storm and the flow of HYSPLIT back trajectory though the storm at approximately 400 hPa. Ozone and its precursors are lifted from the PBL into the upper troposphere by the storm's strong updrafts, while clean air is brought down by downdrafts.

[42] During the early morning sounding on 11 July (Figure 14g), nighttime PBL O_3 is overpredicted by 35 ppbv at the surface. The model is not fully capturing high humidity at the surface (~100%) and ozone depletion through titration and deposition. This may be related to model turbulent

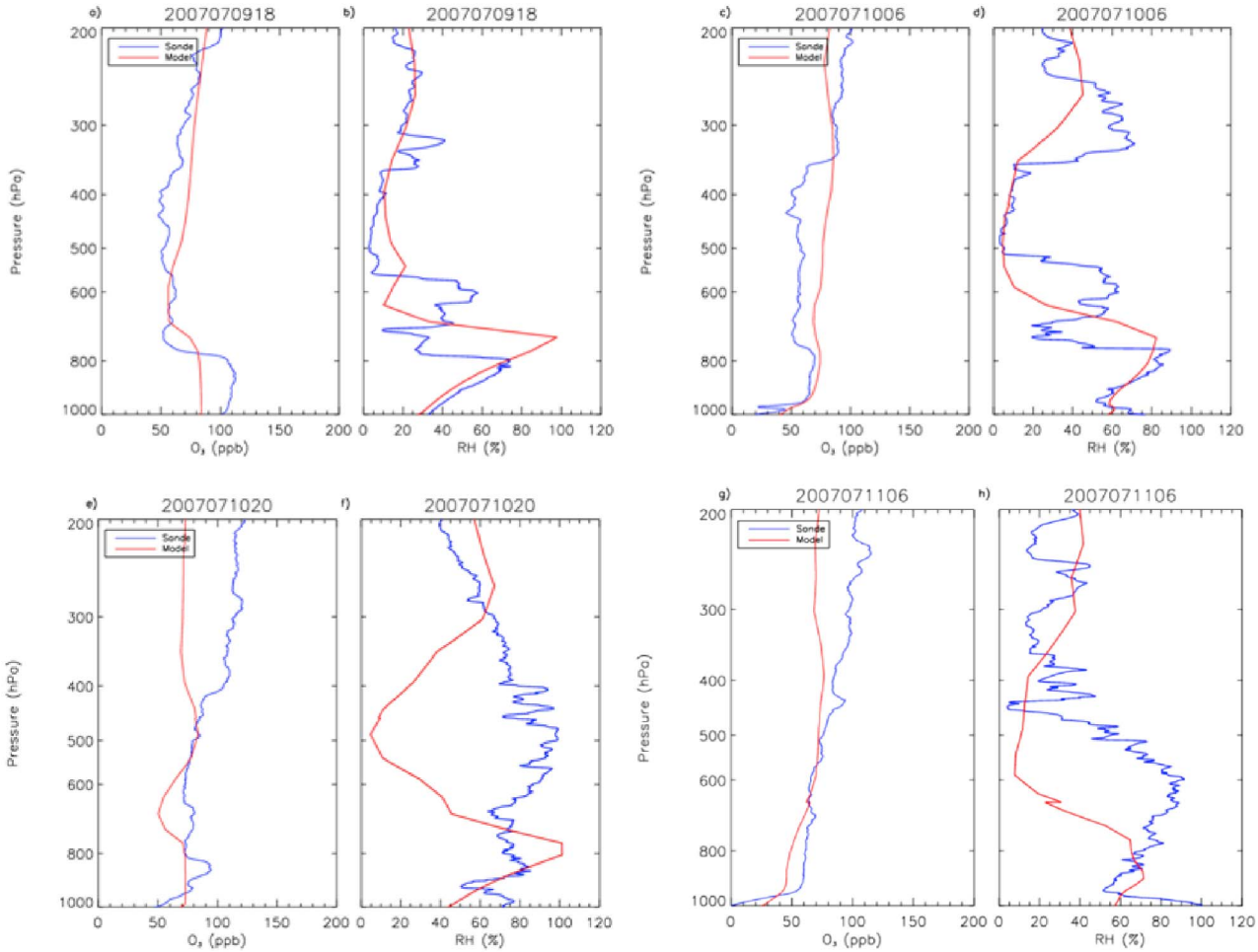

Figure 14. Simulated and observed (a, c, e, and g) ozone and (b, d, f, and h) relative humidity on 9 July 2007 18:00 UTC (Figures 14a and 14b), 10 July 2007 06:00 UTC (Figures 14c and 14d), 10 July 2007 20:00 UTC (Figures 14e and 14f), and 11 July 2007 06:00 UTC (Figures 14g and 14h) at Beltsville, Maryland. WRF/Chem smoothes over much of the fine structure in the boundary layer but generally captures the general vertical profile.

mixing being too fast. The model underpredicts upper tropospheric ozone above 400 hPa by 20–40 ppbv and does not capture observed relative humidity variability.

8. Summary

[43] We have examined model performance in simulating a severe smog episode of July 2007 in eastern United States using surface trace gas observations from EPA AQS, Pinnacle State Park, Great Smoky Mountains, SEARCH stations, and ozonesondes from Beltsville, Maryland. Modeled 8 h O_3 daily maxima suggest that WRF/Chem simulates well the onset and dissipation of the smog event. The model simulates correctly the spatial pattern of surface ozone over most of the domain. Mean bias, root mean square error and correlation coefficient (r) from WRF/Chem 8 h O_3 maximum and observations during 6–11 July 2007 were 0.59 ± 11.0 ppbv, 11.0 ppbv, and 0.7, respectively. However, the low mean biases are a result of underpredicted high O_3 mixing ratios in the northeast and overpredicted moderate O_3 mixing ratios in the southeast. The model had the greatest hit rate of 48.6% on 9 July and averaged 30.2% false alarm ratio over the simulated period.

[44] WRF/Chem captures mean ozone mixing ratios, but shows less variability than is observed, and the model underestimated the magnitude of the 8 h maxima seen on 9 July 2007 in the densely populated northeast. WRF/Chem shows a high bias of 6–11 ppbv in the southeast United States over the course of the smog event, but most of the bias is for observed O_3 mixing ratios less than 40 ppbv. Comparison at individual sites showed that the model captures the diurnal variations in O_3 and passage time of the cold front. In our simulation, WRF/Chem underpredicts daytime O_3 at rural Pinnacles, New York, and Great Smokies, Tennessee, sites and suburban Aldino, Maryland, AQS site. In JST and YRK, Georgia, sites (outside the episode area) daytime and nighttime O_3 are overpredicted. In a separate run, 3-D analysis nudging increased surface ozone biases by 12 ppbv in the southeast United States. This is attributed to increased insolation and temperature in the FDDA run.

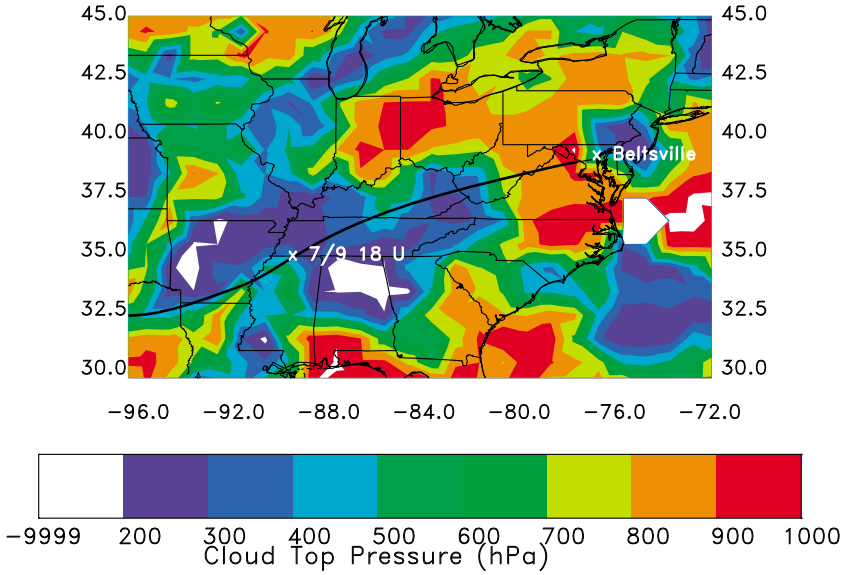

Figure 15. HYSPLIT back trajectories started at 10 July 20:00 UTC at 400 hPa from Beltsville, Maryland. MODIS cloud top pressure on 9 July 18:00 UTC is overlaid to show the airflow through convection over Tennessee, Alabama, and Mississippi prior to arrival in Maryland. Cloud top pressures in unshaded (white) regions are missing data due to high reflectivity of high clouds.

[45] The RAMD2 chemical mechanism used in this simulation does not account for organic coatings that can reduce the accommodation coefficient of wet aerosols for N_2O_5 nor does it include NO_x lifetime-extending reservoir species organonitrates and nitryl chloride. For future work, the lifetime of NO_x in model could be tuned (by adjusting reaction rates within known uncertainties, for example) to match observations, but additional observations of alkyl nitrates and other NO_y species would help develop a more accurate and explicit chemical mechanism. In sensitivity simulation where heterogeneous production of HNO_3 was eliminated to simulate the maximum effect of recycling of NO_x, daytime O_3 mean biases at Aldino, Pinnacles and Great Smokies sites were reduced by 3–5 ppbv. Improvements were seen at other sites as well especially in the polluted northeast. Biases did increase at some sites especially in the southeast where O_3 amounts were low and the base simulation showed a high bias. Another sensitivity simulation showed that too low O_3 dry deposition velocities may contribute to insufficient nighttime depletion of O_3 at SEARCH sites and Aldino, Maryland. Nighttime overprediction of O_3 at these sites could also be caused by overestimation of vertical mixing and/or insufficient titration of O_3 by NO.

[46] Analysis of Beltsville ozonesondes showed that the model captures the vertical distribution of ozone up to 600 hPa, but overestimates mid to upper tropospheric ozone mixing ratios. Daytime underestimation of surface O_3 is attributed to overestimated boundary layer height in the model. The overprediction of nighttime O_3 is attributed to a high vertical mixing coefficient in the model. Modeled relative humidity profiles are in good agreement with observations below 800 hPa. While the model has difficulty capturing subgrid-scale convection events, contributing to local redistribution of trace gases, the general signature of the pollution event is captured well. The model-simulated ozone plume extends into the 815 hPa pressure layer, a portion of the troposphere where ozone information can be retrieved from satellite measurements [*Liu et al.*, 2009]. Since the lowest portion of the free troposphere and the boundary layer are not easily measured from space, WRF/Chem can be used for interpreting the satellite measured tropospheric column ozone in the context of a major surface pollution event. The focus of a follow-up paper will be interpretation of satellite observations of O_3 and its precursors in the northeast United States during this severe smog episode using WRF/Chem.

[47] **Acknowledgments.** The authors acknowledge G. Grell and S. Peckham for help with the WRF/Chem model; L. Emmons for providing MOZART-4 model output; and M. Woodman and D. Krask of the Maryland Department of the Environment's Ambient Air Monitoring Program for support and for providing the Beltsville ozonesonde data and Aldino, Maryland, data, respectively. We thank the anonymous reviewers for their contribution to this work.

References

Allen, D., et al. (2009), Analysis of a summertime air pollution episode with a new dry deposition velocity scheme, paper presented at WRF Users' Workshop, NCAR, Boulder, Colo.

Blanchard, C., and S. Tanenbaum (2006), Weekday/weekend differences in ambient air pollutant concentrations in Atlanta and the southeastern United States, *J. Air Waste Manage. Assoc.*, *56*, 271–284.

Bloomer, B. J., J. W. Stehr, C. A. Piety, R. J. Salawitch, and R. R. Dickerson (2009), Observed relationships of ozone air pollution with temperature and emissions, *Geophys. Res. Lett.*, *36*, L09803, doi:10.1029/2009GL037308.

Brown, S. S., et al. (2006), Variability in nocturnal nitrogen oxide processing and its role in regional air quality, *Science*, *311*, 67–70, doi:10.1126/science.1120120.

Cai, C., et al. (2008), Performance evaluation of an air quality forecast modeling system for a summer and winter season–Photochemical oxidants and their precursors, *Atmos. Environ.*, *42*, 8585–8599, doi:10.1016/j.atmosenv.2008.08.029.

Castellanos, P., L. Marufu, B. Doddridge, B. Taubman, J. Schwab, J. Hains, S. Ehrman, and R. Dickerson (2011), Ozone, nitrogen oxides, and carbon monoxide during pollution events over the eastern United States: An eval-

uation of emissions and vertical mixing, *J. Geophys. Res.*, *116*, D16307, doi:10.1029/2010JD014540.

Crutzen, P. J. (1979), The role of NO and NO_2 in the chemistry of the troposphere and stratosphere, *Annu. Rev. Earth Planet. Sci.*, *7*, 443–472, doi:10.1146/annurev.ea.07.050179.002303.

Dickerson, R. R., et al. (1987), Thunderstorms: An important mechanism in the transport of air pollutants, *Science*, *235*(4787), 460–465, doi:10.1126/science.235.4787.460.

Eder, B., et al. (2009), A performance evaluation of the National Air Quality Forecast Capability for the summer of 2007, *Atmos. Environ.*, *43*, 2312–2320, doi:10.1016/j.atmosenv.2009.01.033.

Emmons, L. K., et al. (2010), Description and evaluation of the Model for Ozone and Related chemical Tracers, version 4(MOZART-4), *Geosci. Model Dev.*, *3*, 43–67, doi:10.5194/gmd-3-43-2010.

Frost, G. J., et al. (2006), Effects of changing power plant NO_x emissions on ozone in the eastern United States: Proof of concept, *J. Geophys. Res.*, *111*, D12306, doi:10.1029/2005JD006354.

Gilliland, A. B., et al. (2008), Dynamic evaluation of regional air quality models: Assessing changes in O3 stemming from changes in emissions and meteorology, *Atmos. Environ.*, *42*, 5110–5123, doi:10.1016/j.atmosenv.2008.02.018.

Godowitch, J. M., A. B. Gilliland, R. R. Draxler, and S. T. Rao (2008), Modeling Assessment of point source NO_x emission reductions on ozone air quality in the eastern United States, *Atmos. Environ.*, *42*, 87–100, doi:10.1016/j.atmosenv.2007.09.032.

Grell, G. A., et al. (2005), Fully coupled "online" chemistry within the WRF model, *Atmos. Environ.*, *39*, 6957–6975, doi:10.1016/j.atmosenv.2005.04.027.

Henderson, B. H., et al. (2011), Evaluation of simulated photochemical partitioning of oxidized nitrogen in the upper troposphere, *Atmos. Chem. Phys.*, *11*, 275–291, doi:10.5194/acp-11-275-2011.

Kang, D., and B. Elder (2005), The New England air quality forecasting pilot program: Development of an evaluation protocol and performance benchmark, *J. Air Waste Manage. Assoc.*, *55*, 1782–1796.

Kuhns, H. D., et al. (2004), Remote sensing of PM, NO, CO and HC emission factors for on-road gasoline and diesel engine vehicles in Las Vegas, NV, *Sci. Total Environ.*, *322*, 123–137, doi:10.1016/j.scitotenv.2003.09.013.

Liu, X., et al. (2009), Ozone profile retrievals from the Ozone Monitoring Instrument, *Atmos. Chem. Phys. Discuss.*, *9*, 22,693–22,738, doi:10.5194/acpd-9-22693-2009.

Loughner, C. P., D. J. Allen, K. E. Pickering, R. R. Dickerson, D.-L. Zhang, and Y.-X. Shou (2011), Impact of fair-weather cumulus clouds and the Chesapeake Bay breeze on pollutant transport and transformation, *Atmos. Environ.*, *45*, 4060–4072, doi:10.1016/j.atmosenv.2011.04.003.

Mao, H., et al. (2010), A comprehensive evaluation of seasonal simulations of ozone in the northeastern U.S. during summers of 2001–2005, *Atmos. Chem. Phys.*, *10*, 9–27, doi:10.5194/acp-10-9-2010.

Parrish, D. D. (2006), Critical evaluation of US on-road vehicle emissions inventory, *Atmos. Environ.*, *40*, 2288–2300, doi:10.1016/j.atmosenv.2005.11.033.

Pickering, K. E., A. M. Thompson, J. R. Scala, W.-K. Tao, R. R. Dickerson, and J. Simpson (1992), Free tropospheric ozone production following entrainment of urban plumes into deep convection, *J. Geophys. Res.*, *97*(D16), 17,985–18,000, doi:10.1029/92JD01716.

Poulida, O., K. L. Civerolo, and R. R. Dickerson (1994), Observations and tropospheric photochemistry in central North Carolina, *J. Geophys. Res.*, *99*(D5), 10,553–10,563, doi:10.1029/94JD00404.

Ryan, W. F., et al. (2000), Air quality forecasts in the mid-Atlantic region: Current practice and benchmark skill, *Weather Forecast.*, *15*(1), 46–60, doi:10.1175/1520-0434(2000)015<0046:AQFITM>2.0.CO;2.

Schwab, J. J., et al. (2009), Ozone, trace gas, and particulate matter measurements at rural site in southwestern New York State: 1995–2005, *J. Air Waste Manage. Assoc.*, *59*, 293–309, doi:10.3155/1047-3289.59.3.293.

Stockwell, W. R., et al. (1990), The second generation Regional Acid Deposition Model chemical mechanism for regional air quality modeling, *J. Geophys. Res.*, *95*(D10), 16,343–16,367, doi:10.1029/JD095iD10p16343.

Talbot, R., et al. (2005), Diurnal characteristics of surface-level O_3 and other important trace gases in New England, *J. Geophys. Res.*, *110*, D09307, doi:10.1029/2004JD005449.

Tanrikulu, S., D. R. Stauffer, N. L. Seaman, and A. J. Ranzieri (2000), A field-coherence technique for meteorological field-program design for air quality studies. Part II: Evaluation in the San Joaquin Valley, *J. Appl. Meteorol.*, *39*, 317–334, doi:10.1175/1520-0450(2000)039<0317:AFCTFM>2.0.CO;2.

Thornton, J., et al. (2010), A large atomic chlorine source inferred from mid-continental reactive nitrogen chemistry, *Nature*, *464*, 271–274, doi:10.1038/nature08905.

Umeda, T., and P. T. Martien (2002), Evaluation of a data assimilation technique for a mesoscale meteorological model used for air quality modeling, *J. Appl. Meteorol.*, *41*, 12–29, doi:10.1175/1520-0450(2002)041<0012:EOADAT>2.0.CO;2.

Wang, W., et al. (2009), *Weather Research and Forecasting ARW Users Manual*, 310 pp., NCAR, Boulder, Colo.

Wesely, M. L., and B. B. Hicks (2000), A review of the current status of knowledge on dry deposition, *Atmos. Environ.*, *34*, 2261–2282, doi:10.1016/S1352-2310(99)00467-7.

Wu, Z., et al. (2011), Evaluating the calculated dry deposition velocities of reactive nitrogen oxides and ozone from two community models over a temperate deciduous forest, *Atmos. Environ.*, *45*, 2663–2674, doi:10.1016/j.atmosenv.2011.02.063.

Yorks, J. E., et al. (2009), The variability of free tropospheric ozone over Beltsville, Maryland (39N, 77W) in the summers 2004–2007, *Atmos. Environ.*, *43*, 1827–1838, doi:10.1016/j.atmosenv.2008.12.049.

Yu, S., R. Mathur, K. Schere, D. Kang, J. Pleim, and T. L. Otte (2007), A detailed evaluation of the Eta-CMAQ forecast model performance for O_3, its related precursors, and meteorological parameters during the 2004 ICARTT study, *J. Geophys. Res.*, *112*, D12S14, doi:10.1029/2006JD007715.

Zhang, D.-L., Y.-X. Shou, and R. R. Dickerson (2009), Upstream urbanization exacerbates urban heat island effects, *Geophys. Res. Lett.*, *36*, L24401, doi:10.1029/2009GL041082.

Zhang, Y., et al. (2006), A comprehensive performance evaluation of MM5-CMAQ for the summer 1999 Southern Oxidants Study episode–Part II: Gas and aerosol predictions, *Atmos. Environ.*, *40*, 4839–4855, doi:10.1016/j.atmosenv.2005.12.048.

D. J. Allen, R. R. Dickerson, and K. E. Pickering, Department of Atmospheric and Oceanic Science, University of Maryland, College Park, MD 20742, USA.

C. P. Loughner and E. A. Yegorova, Earth System Science Interdisciplinary Center, University of Maryland, College Park, MD 20742, USA. (elena.a.yegorova@nasa.gov)